Role of the Interleukin-2 pathways in hepatic innate lymphoid cells during steady state, fibrosis and hepatocellular carcinoma

---

Dissertation

Zur Erlangung des Grades

Doktor der Naturwissenschaften

Am Fachbereich Biologie

Der Johannes Gutenberg-Universität Mainz

Christian Hessel

geb. am 15. August 1987 in Mainz

Mainz, 2021

Dekan: [redacted]

1. Berichterstatter: [redacted]

2. Berichterstatter: [redacted]

Tag der mündlichen Prüfung:

Table of Content

Abbreviations

α-SMA	alpha-smooth muscle actin
(Number)°C	Degree in Celsius
AF(number)	Alexa Fluor
ALD	Alcoholic liver disease
ALP	Alkaline phosphatase
ALT	Alanine aminotransferase
APC	Allophycocyanin
Arm. Hamster	Armenian Hamster
ASH	Alcoholic steatohepatitis
AST	Aspartate aminotransferase
B cell	Bursa of Fabricius-derived cell
BV(number)	Brilliant Violet
CCL2	Chemokineligand 2
CCl_3	Trichloromethyl
CCl_4	Carbon tetrachloride
CD	Cluster of differentiation
CD-HFD	Choline-deficient high-fat diet
CHILP	Common helper-like innate lymphoid cell precursor
CILP	Common innate lymphoid cell precursor
CLP	Common lymphoid progenitor
CTL	Cytotoxic lymphocyte
Cy(number)	Cyanine
DAMP	Danger-associated molecular pattern
DC	Dendritic cell
DMEM	Dulbecco´s modified Eagle´s medium
DNase	Deoxyribonuclease

DTA	Diphtheria toxin A
ECM	Extracellular matrix
ef(number)	efluor
FACS	Fluorescence-activated cell sorting
FCS	Fetal calf serum
FITC	Fluorescein isothiocyanate
FLT3	Fms-like tyrosine kinase 3
Foxp3	Forkhead-Box-Protein P3
FSC-A, -W	Forward scatter area, width
GGT	Gamma-glutamyl transpeptidase
Gr	Granulocyte
H&E	Hematoxylin and eosin
HBV	Hepatitis B virus
HC	High carb
HCC	Hepatocellular carcinoma
HCV	Hepatitis C virus
HEPES	4-(2-hydroxyethyl)-1-piperazineethanesulfonic acid
HFD	High-fat diet
HFHC	High-fat high-carb
HSC	Hepatic stellate cell
ID2	Inhibitor of DNA binding 2
IFNγ	Interferon gamma
IgG	Immunoglobulin G
IHC	Immunohistochemistry
IL(number)	Interleukin
ILC(number)	Innate lymphoid cell
iNOS	Inducible nitric oxide synthase

KC	Keratinocyte
KLRG1	Killer cell lectin-like receptor G1
KO	Knockout
LDH	Lactate dehydrogenase
LTi	Lymphoid tissue inducer cell
MCMV	Mouse cytomegalovirus
MCP-1	Monocyte chemoattractant protein-1
MDSC	Myeloid-derived suppressor cell
MHC-II	Major histocompatibility complex II
MMP(number)	Matrix metalloprotease
MP	Macrophage
N.a.	Not available
NAFLD	Non-alcoholic fatty liver disease
NASH	Non-alcoholic steatohepatitis
NCD	Normal chow diet
NCR	Natural cytotoxicity receptor
NK	Natural killer cell
NKP	Natural killer cell precursor
NKT	Natural killer T cell
NS	Not significant
PAMP	Pathogen-associated molecular pattern
PE	Phycoerythrin
PerCP	Peridinin-chlorophyll protein complex
PMA	Phorbol 12-myristate 13-acetate
RA	Rheumatoid arthritis
ROR	Retinoic acid-related orphan receptor
RPMI	Roswell Park Memorial Institute

RT	Room temperature
SD	Standard deviation
SEM	Standard error of means
SLE	Systemic lupus erythematous
SS	Sjögren syndrome
SSC-A, -W	Side scatter area, width
ST2	Suppressor of tumorigenicity 2
Syr. Hamster	Syrian Hamster
T cell	Thymus-derived lymphocyte
TAA	Thioacetamide
TCR	Thymus-derived lymphocyte receptor
TG	Triglyceride
TGF	Transforming growth factor
$T_{H(number)}$	Helper Thymus-derived lymphocyte
TIMP- 1	Tissue inhibitor of metalloproteases-1
TNF	Tumor necrosis factor
Treg	Regulatory thymus-derived lymphocyte
VAT	Visceral adipose tissue
WT	Wildtype

Figures

Tables

1 Zusammenfassung

Das Immunsystem ist ein essenzieller Teil unseres Körpers da es dafür verantwortlich ist verschiedene Gefahren wie Viren oder Bakterien abzuwehren. Gleichzeitig benötigt es eine genaue Regulierung, da eine übermäßige oder falsch ausgerichtete Immunantwort gesunde Zellen und Organe schädigen kann. Diese Regulation erfolgt unter anderem durch Zytokine. Eine wichtige Rolle spielt dabei Interleukin- (IL)2, welches z.B. von „cluster of differentiation“ (CD)4 T Zellen sekretiert und von regulatorischen CD4 T Zellen (Treg) konsumiert wird, beides Zellen des adaptiven Immunsystems (Gordon et al., 1965). Erst kürzlich wurde auch eine Funktion in der Regulation von Zellen des innaten Immunsystems, hier „natural killer“ (NK) Zellen und „innate lymphoid cells“ (ILC)1 (Gruppe 1 ILCs) beschrieben (Gasteiger, Hemmers, Bos, et al., 2013; Gasteiger, Hemmers, Firth, et al., 2013). Die genaue Funktion und Wirkungsweise von IL2 auf diese Zelltypen ist weitgehend unbekannt. Ziel dieser Arbeit war es, vor allem durchflusszytometrische Methoden für die Analyse hepatischer Immunzellen, mit Fokus auf Gruppe 1 ILCs, zu etablieren. Als Modelle wurden Diät- und Toxin-induzierte Lebererkrankungen gewählt. Zusätzlich sollte die Rolle von Gruppe 1 ILCs in diesen Modellen anhand von genetisch veränderten Mäusen charakterisiert werden. IL2 und seine Rezeptor Untereinheit CD25 wurden auf ihr Potenzial die Gruppe 1 ILC vermittelte Immunantwort in konditional depletierten Mäusen zu regulieren untersucht. Es konnte gezeigt werden, dass ILC1s in verschiedenen Langzeitmodellen von Leberfibrose CD25 vermehrt produzieren. Dafür wurden die experimentellen Modelle der Cholin-defizienten Fettdiät (CD-HFD), einer Kohlenhydrat- und Fettdiät, sowie der Tetrachlormethan (CCl_4)- und Thioacetamid (TAA)-induzierten Leberfibrose verwendet. Für die Versuche wurden wildtyp Mäuse oder Mäuse, deren Gruppe 1 ILCs depletiert sind oder in denen diese kein IL2 oder CD25 mehr herstellen können, verwendet. Gruppe 1 ILCs von wildtyp Mäusen zeigten eine höhere Fraktion von $Ki67^+$ Zellen unter CD-HFD wobei diese Zellen gleichzeitig weniger Zytokine (Interferon gamma (IFNγ), Tumornekrosefaktor alpha (TNFα) und IL2) produzierten. Die Depletion von Gruppe 1 ILCs führte zu einer geringeren Inflammation und einer erhöhten Rate an M2-ähnlichen Makrophagen unter CD-HFD. Vermehrte M2-ähnliche Makrophagen, Granulozyten und dendritische Zellen waren auch in der Heilungs-Phase der CCl_4-induzierten Leberfibrose zu erkennnen. Die Depletion von CD25 auf Gruppe 1 ILCs führte zu einer geringeren IL2 Produktion dieser Zellen, wobei die generelle IL2 Produktion dieser Zellen unter CCl_4-induzierter

Leberfibrose stark verringert war. Die spezifische genetische Depletion des IL2 Gens in NK Zellen und ILC1 führte zu erhöhten Frequenzen von M2-ähnlichen Makrophagen in der akuten Phase und erhöhten Frequenzen von M1-ähnlichen Makrophagen in der Heilungs-Phase von CCl_4-induzierter Leberfibrose. Um die Rolle von Matrixmetalloproteasen (MMP) auf den Verlauf der Leberfibrose herauszufinden wurden Versuche mit MMP3-depletierten Mäusen gemacht, die zeigten, dass ILC1s eine veränderte Rate an $Ki67^+$ Zellen und $CD25^+$ Zellen in der akuten und der Heilungs-Phase von CCl_4-induzierter Leberfibrose aufweisen. Die Ergebnisse zeigen eine vielfältige Rolle von IL2, produziert von Gruppe 1 ILCs, und der Zellpopulation der Gruppe 1 ILCs in der akuten Phase der Leberfibrose und der Heilungs-Phase.

2 Summary

The immune system is an essential part of our body that is able to combat diverse attacks like viruses, bacteria and tumor cells. At the same time it needs a tight regulation as an overwhelming immune response can harm healthy cells and organs whereas an improper immune response can lead to the spread of invading pathogens within the body. Cytokines are able to regulate immune responses. One of them, namely interleukin- (IL)2, is mainly secreted by cluster of differentiation (CD)4 T cells and consumed by regulatory T cells (Tregs), both cell compartments of the adaptive immune system (Gordon et al., 1965). It was just recently described that IL2 can also act on cells of the innate immune system, mainly group 1 innate lymphoid cells (ILCs) (Gasteiger, Hemmers, Bos, et al., 2013; Gasteiger, Hemmers, Firth, et al., 2013). The exact role of IL2 on group 1 ILCs still remains largely unknown. The aim of this thesis was to establish mainly flow cytometric methods to study hepatic immune cells, herewith especially group 1 ILCs, in the course of diet- and toxin-driven liver disease models. Additionally, the role of group 1 ILCs within these models should be characterized with the help of genetic mouse models. IL2 and its receptor subunit CD25 were studied in regard of their potential to regulate the group 1 ILC-mediated immune response in conditional knockout mice. It can be shown that in different long-term models of liver fibrosis ILC1s upregulated CD25. Models investigated are choline-deficient high-fat diet (CD-HFD), high-fat high-carb (HFHC) diet and carbon tetrachloride (CCl_4)- and thioacetamide (TAA)-induced liver fibrosis. We performed these experiments with wildtype (WT) mice and genetic knockouts (KOs) specifically depleting either IL2 or CD25 in natural killer (NK)p46$^+$ group 1 ILCs. Group 1 ILCs showed a higher proliferation after long-term CD-HFD and at the same time produced less cytokines like interferon gamma (IFNγ), IL2 and tumor necrosis factor alpha (TNFα). Unexpectedly, depletion of group 1 ILCs led to reduced inflammation and increased anti-inflammatory M2-like macrophages (MPs) during CD-HFD and an increase in M2-like MPs, granulocyte (Gr)1$^+$ cells and DCs in the reversal phase of CCl_4-induced liver fibrosis. Depletion of CD25 in group 1 ILCs led to a slight increase in IL2 production from ILC1s whereas the overall production of IL2 by ILC1s tremendously decreased after CCl_4-induced liver fibrosis. Therefore, IL2-depletion on group 1 ILCs seems to affect mainly the innate immune cell compartment. M2-like MPs increase during the acute phase of CCl_4-induced liver fibrosis whereas M1-like MPs increase during the reversal phase. Further experiments focused on the role of matrix

metalloproteases (MMPs) for ILC1 function. MMP3 KO mice showed altered proliferation and CD25 expression of ILC1s during the acute and reversal phase of CCl_4-induced liver fibrosis. In summary, the presented work highlights diverse roles of ILC1s and ILC-derived IL2 during the acute phase of liver fibrosis and in the tissue healing phase.

3 Introduction

3.1 Innate and adaptive interaction of the immune system

The immune system protects the body from pathogens coming from the environment and from own, transformed cells. At the same time, it needs a tight regulation as the cytotoxic features can harm healthy and important cells and tissue .The acute killing of invading pathogens is mainly done by the innate arm of the immune system, consisting mainly of neutrophils, macrophages (MPs), dendritic cells (DCs) and natural killer cells (NKs) (Figure 1). The adaptive arm is responsible for creating memory within the immune system that protects from a reinfection with a previously encountered pathogen. This compartment is mainly established by T cells, that recognize antigens specifically via their T cell receptor (TCR), and B cells, that produce antibodies to mark pathogens that can be destroyed by phagocytes and others. A subset of cluster of differentiation (CD)4^+ T cells, FoxP3^+CD25^+ regulatory T cells (Tregs) keep the innate and adaptive immunity in check. They prevent an overwhelming immune response by secreting interleukin (IL)10 and transforming growth factor beta (TGF-β). If depleted genetically, mice develop a severe autoimmune disease (J. M. Kim et al., 2007). Their ability to suppress immune cells can also limit a proper response against malignant cells. Depletion of Tregs in tumors improves the anti-tumor response by a higher IL2 production of CD25^-CD4^+ T cells and an enhanced activity of CD8^+ cytotoxic lymphocytes (CTLs). Furthermore, IL2 activates NK cells to improve the anti-tumor response (Shimizu et al., 1999). The IL2 pathway has been considered as an interesting target for immunotherapy. IL2 was the first cytokine being discovered in the 1960´s and back then already described as a soluble factor secreted by lymphocytes, promoting their proliferation (Gordon et al., 1965). Until today, it is ubiquitously used in *in vitro* cultures to ensure the proliferation of T cells and NK cells. However, the exact mechanism of production, regulation and spatiotemporal availability *in vivo* is still a subject of intense studies. IL2 signals via the IL2 receptor, which consists of IL2Rα (CD25), IL2Rβ (CD122) and IL2Rγ (CD132, also known as common gamma chain receptor). The CD122 receptor domain is shared with IL2 and IL15 and CD132 is shared with IL2, IL4, IL7, IL9 and IL15. The heterodimeric complex of CD122 and CD132 can also signal for IL2 on its own but only has a low affinity. Once the trimeric receptor is completed with CD25, it can signal with high affinity. CD25 is expressed on Tregs and other activated lymphocytes like B cells, CD4^+ T cells, DCs and ILC1s (Gasteiger, Hemmers, Bos, et al., 2013; Li et al., 2016). On innate lymphoid cells type

1 (ILC1s), it can be induced by IL12 and IL18 stimulation, for example being released after mouse cytomegalovirus (MCMV) infection (Lee et al., 2012). Being in close proximity to an IL2 producer in the tissue might provide help for NK cells to proliferate and kill viruses. So far, it is known that Tregs cannot produce IL2, being dependent on CD4 effector T cells or others to provide it. Due to their high CD25 expression, Tregs are the major consumers. Other reported producers of IL2 are DCs (Granucci et al., 2003). They seem to provide an early source of IL2 during the innate immune response after microbial encounter. Another way of signaling for IL2 is by trans-presentation of CD25 by a neighboring cell. This was shown for DCs to trans-present the receptor for IL2 (human *in vitro* data), IL15 and IL6, mainly to T cells or NK cells, which also seems to be a relevant and often overlooked way to regulate the microenvironment of cells (Castillo et al., 2009; Heink et al., 2017; Wuest et al., 2011).

The fact that CD25 can be secreted by the cells as a soluble factor makes the exact mechanism of regulation even more difficult to investigate. The secretion of CD25 by different cells made it attractive to use as a general marker being increased in several diseases like systemic lupus erythematosus (SLE), rheumatoid arthritis (RA) and cancer, characterizing an activated immune system (Campen et al., 1988; Murakami, 2004; R. E. Wolf et al., 1988). An *in vitro* study also showed that soluble CD25 can bind IL2, thereby adding another mechanism to regulate the availability to IL2 (Rubin et al., 1986). A cell-type specific deletion of the receptor or the cytokine might bring new insights into the complex signaling cascade and new targets to improve the immune response against tumors, viruses and bacteria.

A recently discovered cell compartment are ILCs (Figure 1). They are categorized due to their effector function of releasing certain cytokines in group 1, 2 and 3 ILCs (Spits et al., 2013). The previously mentioned NK cells, mainly producing interferon gamma (IFNγ), belong to the group 1 ILCs, together with ILC1s, that produce IFNγ, tumor necrosis factor alpha (TNFα) and IL2. NK cells additionally release granzymes to directly kill infected cells. Due to their cytokine profile and transcription factors, ILCs are categorized like T cells, where T_H1 cells release IFNγ and depend on Tbet. T_H2 cells, or ILC2s, representing the group 2 ILC compartment, mainly release IL4, IL5 and IL13 and rely on the transcription factor GATA3. T_H17 cells or the related group of ILC3s, which also include the lymphoid tissue inducer cells (LTis), are known for their potential to produce IL17, IL21 and IL22 and depend on the transcription factor RORγt.

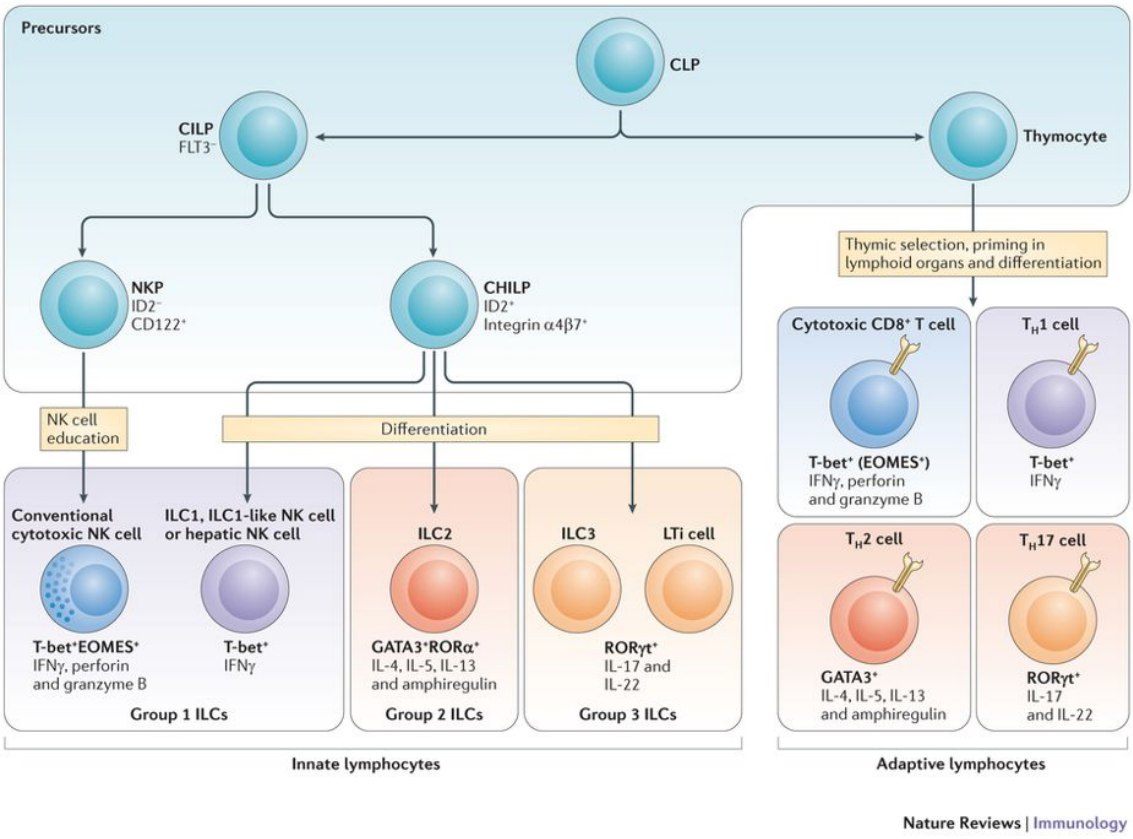

Figure 1: ILC and T cell lineages

Both cell compartments share the common lymphoid progenitor (CLP). Thymocytes undergo thymic selection and develop in lymphoid organs into T_H1, T_H2 or T_H17 cells. ILCs share the common innate-like precursor cells that develops into an conventional NK cell precursor (NKP) or a common helper-like innate precursor (CHILP). From there, they differentiate into ILC2, ILC3 or LTi cells. All cell compartments have their signature cytokine profile and transcription factor (Figure adapted from Gasteiger et al., 2014).

The balance between the innate and adaptive immune system needs a tight regulation as a misbalance can lead to tissue damage and autoimmune diseases or to ineffective immune responses towards harmful pathogens. Another important point for a proper immune response is the location of the cells. ILCs were described to mainly be tissue-resident (Gasteiger et al., 2015). Once they developed from the common helper ILCs (CHILPs) in the bone marrow, they circulate through the body and seed different tissues. Epithelial surfaces that are exposed to environmental factors need a different immune cell compartment than the small intestine, that mainly faces pre-processed food but has to balance the local microbiota and potentially harmful antigens in the food. According to that location-specific requirement for immune cells, group 1 ILCs are mainly found in metabolic active organs like the adipose tissue and the liver. ILC2s are mainly found in the lung and in the skin to guarantee a proper immune response

but in parallel prevent an exceeding one. ILC3s resemble a major fraction of lymphocytes in the small intestine to release effector cytokines and thereby control microbiota and tissue integrity.

3.2 Liver metabolism and disease

The liver is an essential organ in our body that is responsible for many tasks. Its major functions include metabolism of proteins, production of the bile and de-toxification of the body. Due to this multifunctional role, a liver failure is fatal. With the help of the bile, that is produced in the liver and secreted into the small intestine, nutrients from food can be digested and made accessible for the body. The processed nutrients, by then in the form of amino acids are further distributed from the gut into the blood stream and then the liver. Depending on the need for glucose and other molecules, the liver can either synthesize glucose and provide it directly to the body via the blood stream or it can store the excessive amount of glucose as glykogen. The side products of nitrogen are processed into urea that is transported to the kidney, where it leaves the body via the urine. This process helps to prevent a toxification of the body with high nitrogen or ammonium. The fast recovery rate after damage or resection underlines the importance of the liver. Nevertheless, long-term chronic inflammation or continuous damage can harm and destroy the liver (Figure 2). The threats can have multiple sources. One of them is the excessive consumption of alcohol, which is filtered and processed in the liver. Others are the exposure to toxins, viral infections, especially hepatitis B or C, or a metabolic syndrome, caused by a high-fat diet. Continuous damage leads to the accumulation of extracellular matrix (ECM) and the destruction of the liver structure, called fibrosis.

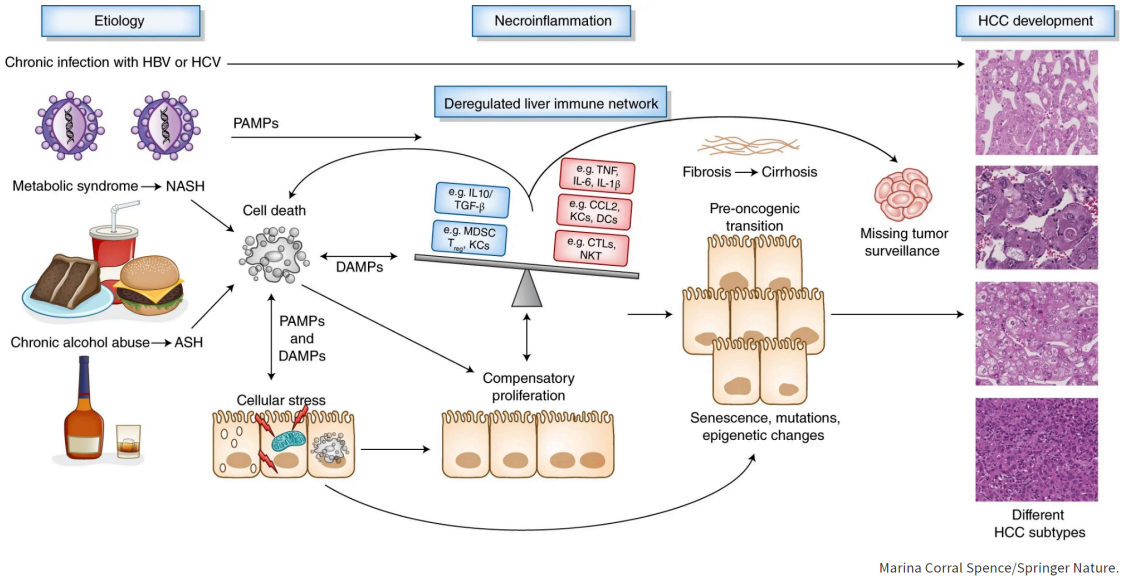

Figure 2: Chronic infections, metabolic syndrome or chronic alcohol abuse can cause liver disease

Cell death, caused by the accumulation of lipids in the cells leads to compensatory proliferation and a misbalance of the liver immune network. Fibrosis, cirrhosis and eventually tumor can develop and lead to phenotypes illustrated as H&E stained liver sections on the right (Figure from M. J. Wolf et al., 2014).

Accumulation of extracellular matrix is caused by wound-healing processes following the damage in the tissue and leading to the formation of scars. The ECM consists of a variety of molecules, for example collagen, growth factors and matrix metalloproteases. It regulates cell differentiation, migration and proliferation (Schuppan et al., 2001). In the case of alcohol being the source of the disease, it is called alcoholic liver disease (ALD). If not, it is called non-alcoholic fatty liver disease (NAFLD). Both are characterized by their clinic pathology of elevated serum markers for liver enzymes, mainly aspartate aminotransferase (AST) and alanine aminotransferase (ALT). A major limitation of the diagnosis is, that a liver biopsy is still the “gold-standard” to precisely determine the type of liver disease. The mainly non-symptomatic course of disease, pain and the invasive method of taking a biopsy lead to the fact that the diseases are often recognized at an developed stage or after routine check-up of the blood. NAFLD can further progress into a state of steatosis, called non-alcoholic steatohepatitis (NASH) (Brunt, 2004). At this stage, the accumulation of lipids, coming from the processed food in the gut, leads to hepatocyte cell death. If not treated, liver damage can progress to cirrhosis. At this stage, the liver loses many of its original functions. Liver cirrhosis can end in failure of the organ or in the

development of hepatocellular carcinoma (HCC). To better understand the processes during the different stages of liver disease, several mouse models were established.

3.3 High-fat diet-induced liver fibrosis and HCC

One of the models that closely recapitulates metabolic syndrome, NASH and NASH-induced HCC is the model of choline-deficient high-fat diet (CD-HFD). High-fat diet (HFD) itself leads to a massive increase in lipid accumulation in the liver. Choline is essential for releasing bile and the transport of triglycerides out of the liver (Corbin et al., 2012). The accumulation of bile in the liver leads to an increased damage and a fast development of NASH and HCC (M. J. Wolf et al., 2014). CD-HFD is characterized by a massive lymphocyte accumulation in the liver. Especially CD4 T cells, Tregs, CD8 T cells, NK cells and myeloid cells are elevated and contribute to steatosis, NASH and HCC development in this model, closely resembling the human disease.

3.4 CCl_4-induced liver fibrosis

Another model to study liver diseases is carbon tetrachloride (CCl_4)-induced liver fibrosis. Here, CCl_4 gets metabolized in the liver, resulting in the new form of trichloromethyl radical (CCl_3*) (Scholten et al., 2015). These radicals can react with nucleic acids, proteins and lipids, leading to the development of inflammation, steatosis and eventually also mutations, which can lead to HCC. CCl_4 can be applied via different routes, preferentially with oral gavage. The long-term treatment can be maintained over several weeks, leading to NASH. Once the treatment stops, the liver recovers and tissue healing processes can be investigated. The liver-specific damage and the relatively short induction time over several weeks, rather than months in the high-fat diet models, are attractive features of CCl_4-induced liver fibrosis. On the other hand, the high-fat diet-induced liver damage is systemic and more physiological due to the lack of toxins inducing the damage. HFD experiments therefore have the advantage of also affecting adipose tissues, which can be studied in parallel to the liver.

3.5 Group 1 ILCs and Tregs in the liver

It was shown before that group 1 ILCs can also play a role in the course of obesity-related diseases, especially in contributing to the effects of a high-fat diet (Wensveen et al., 2015). In the model of HFD, NK cells were shown to produce more IFNγ and

therewith polarize proinflammatory M1-like MPs. Another study confirmed these findings with a similar observation, showing that tissue-resident ILC1s, but nor mature neither immature NK cells contribute to obesity-related pathology by polarizing M1-like proinflammatory MPs via IFNγ after IL12 signaling in adipose tissue (O'Sullivan et al., 2016). Additionally, it was shown that NK cells take up lipids during obesity which limits their cytotoxic capacity. This reduced cytotoxicity also leads to a less effective anti-tumor response (Michelet et al., 2018). Nevertheless, the exact role and the regulation of group 1 ILCs in the development of steatosis, NASH and HCC in the liver still remains elusive. So far, a major limitation was the lack of cell-specific knock-out mice. Many studies were done with depletion experiments that might have secondary effects due to the toxins used for depletion and the acute change in the immune system. Identifying novel regulators of this partly recently discovered cell populations could provide potential therapeutic approaches to combat the vicious circle of liver diseases.

IL2, a mediator between innate and adaptive lymphocytes, might also be involved in the regulation of group 1 ILCs as shown in Figure 3 (Gasteiger et al., 2014). As previously described, group 1 ILCs can sense IL2 and are regulated by Tregs that limit the availability of IL2 by their high CD25 expression (Gasteiger, Hemmers, Bos, et al., 2013; Gasteiger, Hemmers, Firth, et al., 2013).

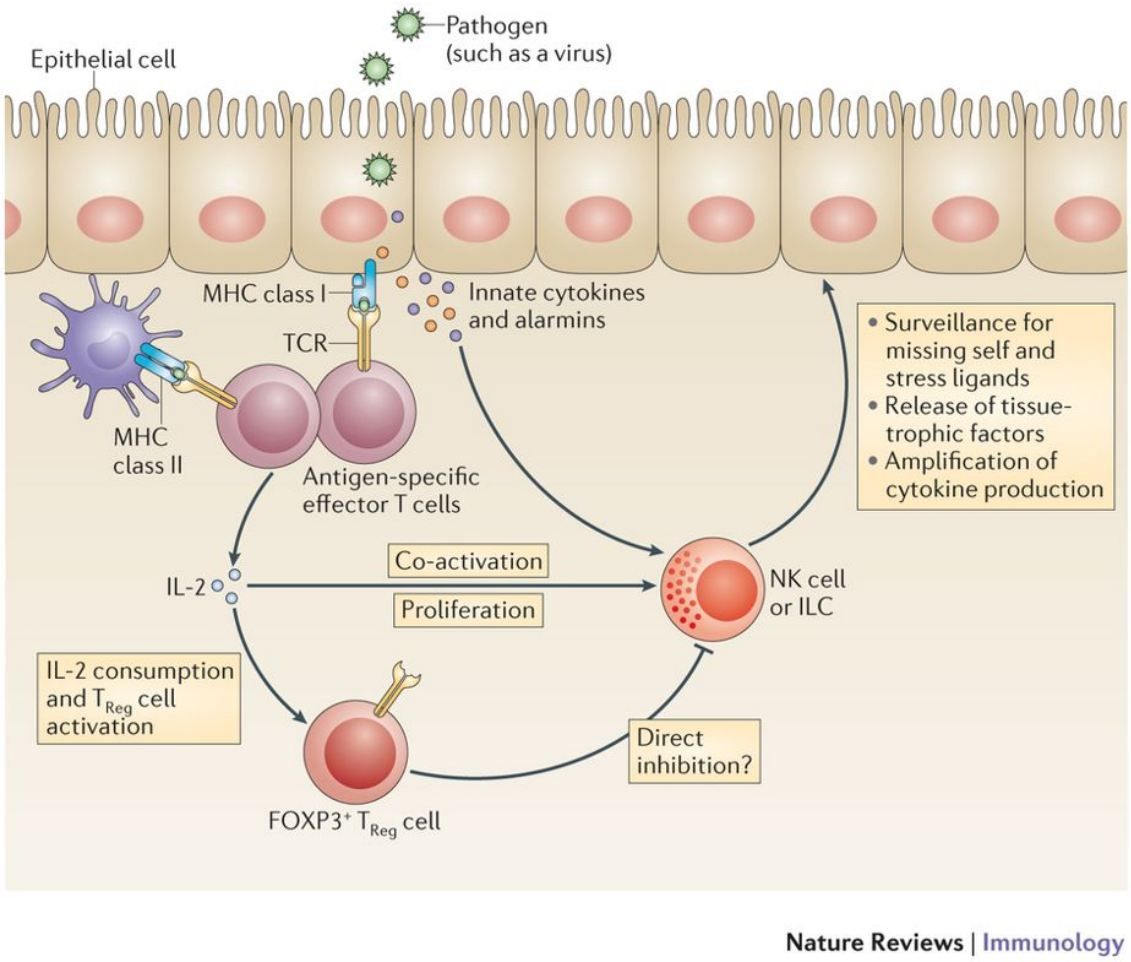

Figure 3: IL2 as a mediator between innate and adaptive lymphocytes

Innate cytokines can directly activate NK cells or ILCs. The access and availability to IL2 can be restricted by Tregs by their high CD25 expression. This regulation can help to keep the balance between a proper immune response against pathogens and immunosuppression to prevent autoimmunity (Figure adapted from Gasteiger et al., 2014).

Tregs also play a role during HFD-induced NASH by expressing less IL10 and a decrease in ST2$^+$ Tregs in visceral adipose tissue (VAT) after a high-fat/sucrose diet (Han et al., 2015). The decrease in ST2$^+$ Tregs and the effects of limited Treg function can be reversed by IL33 administration. IFNγ on the other hand has devastating effects on Tregs and inhibits the IL33 effects to promote Treg proliferation (Deng et al., 2017). As a result, the investigation of IL2 in regulating group 1 ILC compartment might provide new insights into the complex interaction of cells that contribute to liver diseases.

4 Aims of the thesis

A potential role for the IL2-pathways in ILCs has recently been suggested in the spleen and in the gut (Zhou et al., 2019). The aim of this thesis was to investigate the role of the IL2-pathways in hepatic ILC1 during steady state and liver inflammation. To this end, methods should be established in order to study hepatic immune cells in the course of diet- and toxin-driven liver disease models. Next, the role of group 1 ILCs within these models should be characterized with the help of genetic mouse models. Finally, IL2 and its receptor subunit CD25 should be studied using conditional knockout mice in order to understand their potential to regulate local ILC1-mediated immune responses:

Aim 1: Establish methods to analyze the hepatic immune cell compartment, namely innate lymphoid cells, myeloid cells and T cells via flow cytometry.

Aim 2: Study the effect of diet-driven hepatic inflammation and fibrosis on innate lymphoid cells in wildtype mice to get a precise understanding about their role.

Aim 3: Characterize the population dynamics and function of hepatic ILCs in the induction and reversal phases of toxin-driven hepatic fibrosis. Having data from different models available would allow us to better address questions on the regulation of innate lymphoid cells.

Aim 4: Establish and characterize novel genetic mouse models that would allow us to deplete group 1 ILCs, and to deplete IL2 and the IL2 receptor CD25 specifically in group 1 ILCs. These novel models should then be used to dissect the role of group 1 ILCs, and the role of these molecule in group 1 ILCs, for the hepatic immune cell compartment and disease progression in the disease models established and investigated under Aim 2 and 3.

5 Materials & methods

5.1 Chemicals and reagents

Table 1: Chemicals and reagents

Chemical / Reagent	Supplier
123count eBeads	eBioscience, San Diego, USA
Ammonium chloride (NH_4Cl)	Roth, Karlsruhe, Germany
Brefeldin A	Sigma-Aldrich, Steinheim, Germany
CD-HFD (45% kcal% fat without added Choline)	Research Diets, New Brunswick, USA
Collagenase D	Roche, Basel, Switzerland
DMEM	Thermo Fisher Scientific, Waltham, USA
DNAse I from bovine pancreas (50U/ml)	Sigma-Aldrich, Steinheim, Germany
Dulbecco´s modified PBS (DPBS)	Sigma-Aldrich, Steinheim, Germany
Ethylenediaminetetraacetic acid (EDTA)	Roth, Karlsruhe, Germany
Fetal calf serum (FCS)	Sigma-Aldrich, Steinheim, Germany
Fixation/Permeabilization Solution Kit	BD Biosciences, Franklin Lakes, USA
FoxP3 / Transcription Factor Staining Buffer Set	eBioscience, San Diego, USA
HEPES	Sigma-Aldrich, Steinheim, Germany
HFD (45% kcal% Fat)	Research Diets, New Brunswick, USA
IL2 (human, recombinant)	Peprotech, New Jersey, USA
IL12p70 (mouse, recombinant)	Peprotech, New Jersey, USA
IL18 (mouse, recombinant)	R&D Systems, Minnesota, USA
Ionomycin	Sigma-Aldrich, Steinheim, Germany
Percoll	Sigma-Aldrich, Steinheim, Germany
PMA	Sigma-Aldrich, Steinheim, Germany
Potassium bicarbonate ($KHCO_3$)	Sigma-Aldrich, Steinheim, Germany
RPMI-1640 Medium	Thermo Fisher Scientific, Waltham, USA
Sodium chloride (NaCl) infusion bag	Braun, Melsungen, Germany
ß-mercaptoethanol	Applichem, Darmstadt, Germany

5.2 Methods

5.2.1 Mice

All mice used in this study had C57BL/6 background and were housed under specific-pathogen-free conditions either at the mouse facility of the DKFZ in Heidelberg (see results in 6.3) or of the University Medical Center Mainz. All experiments were performed in accordance with the local guidelines and regulations for animal care.

5.2.2 *In vivo* mouse model of CD-HFD

C57BL/6 WT, NKp46Cre x iDTA and NKp46Cre x IL2flox mice, 4-16 weeks old, were fed a CD-HFD containing 45% fat for 6 weeks or up to 12 months. Blood samples were taken every month to track ALT and cholesterol levels. Mice were sacrificed and tissue was harvested for Histology and FACS Analysis.

5.2.3 *In vivo* mouse model of HC/HCHF-induced liver fibrosis

C57BL/6 WT female mice, 7 weeks old at start, were fed a high-fat diet containing 59% fat plus 0.5% cholesterol (HC group) or normal chow diet (control group). Mice of the HCHF group additionally received a glucose/fructose solution in their drinking water, containing 42g/l sugar made of 55% fructose and 45% glucose. Mice were sacrificed after 14 weeks on diet, tissue was harvested for qPCR and FACS Analysis and blood for the analysis of serum parameters.

5.2.4 *In vivo* mouse model of CCl_4- and TAA-induced liver fibrosis

C57BL/6 WT, NKp46Cre x iDTA, NKp46Cre x IL2flox, NKp46Cre x CD25flox, MMP3KO and MMP8KO mice, 4-16 weeks old, were treated with escalating doses of thioacetamide (TAA) or CCl_4 for 6 weeks to induce liver fibrosis (Y. O. Kim et al., 2017). TAA was injected intraperitoneal three times a week, starting with 50 mg/kg (1^{st} and 2^{nd} dose, week 1), 100 mg/kg (2^{nd} to 5^{th} dose, week 1–2), 200 mg/kg (6^{th} to 10^{th} dose, week 2–4), 300 mg/kg (11^{th} to 15^{th} dose, week 4–5), and 400 mg/kg (16^{th} dose onwards, week 6). CCl_4 was administered three times a week by oral gavage 50/50 vol mixed with mineral oil: 0.875 ml/kg (1^{st} dose, week 1), 1.75 ml/kg (2^{nd} to 9^{th} dose, week 1–3) and 2.5 ml/kg (10^{th} to 18^{th} dose, week 4-6). Oral gavage of mineral oil served as control. Animals were sacrificed after 6 weeks of treatment or after 3 weeks of spontaneous reversal, off TAA or CCl4, and tissues were harvested for FACS analysis.

5.2.5 Preparation of single cell suspensions from whole mouse livers

Mice were anesthetized and sacrificed with CO_2 according to the regulations for animal care. Mice were opened on the ventral side, the diaphragm was opened and the right ventricle of the heart was cut open. A 23G needle connected to an infusion bag containing 0,9% sodium chloride in H_2O was inserted to the left atrium of the heart to perfuse the liver. After 1-2 minutes the liver got pale and was cut off the body and put on ice in cold PBS. Livers were cut into small pieces with fine scissors in 4ml of digestion mix (1mg/ml Collagenase D, 20μg/ml DNase and HEPES in DMEM) in a 50ml tube. Tubes were incubated at 37°C for 40 minutes while shaking in a thermoshaker. Digestion was stopped with 20ml PBS + ß-mercaptoethanol being flushed and minced through a 70μm cell strainer. The cells were spun down for 7 minutes at 350g at 4°C. If needed, an aliquot for counting was taken (100μl), the supernatant was discarded and the pellet was resuspended in 7ml of 40% Percoll. 15ml tubes were prepared containing 5ml of 80% Percoll. The 40% Percoll mix with the cells was slowly and carefully pipeted on top of the 5ml 80% Percoll. The tube was spun down at RT with lowest acceleration and no brake at 1300g for 20 minutes. After that the middle layer was suck up (about 3ml in total), transferred into a new 15ml tube and washed with 10ml cold PBS. The tubes were tilted several times to wash off Percoll. Cells were spun down for 7 minutes at 4°C at 300g. The pellet was resuspended in 600μl D10 and cells were used at 100-200μl/staining or stimulation.

5.2.6 Preparation of single cell suspensions from mesenteric lymph nodes and the spleen

Mice were anesthetized and sacrificed with CO_2 according to the regulations for animal care. Mice were opened on the ventral side. The mesenteric lymph nodes (mLN) and the spleen were collected from the body and put on ice in cold PBS. mLN were cut into small pieces with fine scissors in 2ml of ice cold PBS. mLN and spleen were mashed through a 70μm cell strainer. A spin for 5 minutes at 350g led to the formation of a cell pellet which was resuspended in 2ml red blood cell lysis buffer (150 mM NH_4Cl, 10mM $KHCO_3$ and 100μM EDTA (pH 8.0) in H_2O, used for spleen only) and left for incubation for 2 minutes. The cells of mLN or spleen were spun down for 7 minutes at 350g at 4°C. The supernatant was discarded and the pellet was resuspended in 2ml D10. The cells were used at 100-200μl/staining or stimulation.

5.2.7 Cell counting

Cells were prepared as described before and an aliquot of 100µl was taken for counting. 20µl of a 5X concentration of an antibody cocktail containing the surface marker CD45 (and optional CD4, CD8, NK1.1) were added on top. The cells were incubated for at least 15 minutes at 4°C and then diluted with 200µl of Facs buffer containing 3000 counting beads (123 counting beads) and directly acquired on a flow cytometer. With the help of the counting beads total numbers of $CD45^+$ cells and subpopulations were calculated in FlowJo Software.

5.2.8 *In vitro* stimulation assay for intracellular cytokine staining

200µl of the cell suspension prepared in 5.2.5 were seeded in a 96-well U-bottom plate. 50µl of a stimulation cocktail was prepared in a 5X concentration containing PMA, Ionomycin and Brefeldin A, added to the cells and carefully resuspended. The plate was incubated for 4h at 37°C in the incubator. Cells were put on ice for 10 minutes, then thoroughly resuspended and transferred to a V-bottom 96-well plate for antibody staining (see 5.2.10).

5.2.9 *In vitro* stimulation of splenocytes

100µl of the splenocyte suspension prepared in 5.2.6 were seeded in a 96-well flat-bottom plate. 100µl of a stimulation cocktail (IL2 (final concentration 20ng/ml) +/- IL12 (final concentration 10ng/ml) + IL18 (final concentration 10ng/ml)) was prepared in a 2X concentration, added to the cells and carefully resuspended. The plate was incubated for 12h at 37°C in the incubator. Cells were put on ice for 10 minutes, then thoroughly resuspended and transferred to a V-bottom 96-well plate for antibody staining (see 5.2.10).

5.2.10 Flow cytometry and antibodies

Cell suspensions were prepared as described in 5.2.5 or 5.2.8. Cells were transferred to a 96-well V-bottom plate at 100-200µl /well and spun down at 300g for 2 minutes at 4°C. Supernatant was discarded and cells were resuspended in 50µl/well PBS containing live-dead-dye and Fc-block (αCD16/32 Antibody) and incubated for at least 12 minutes. 150µl of Facs buffer (PBS + Sodium Azide + FCS) was added. Cells were spun down at 300g for 2 minutes at 4°C. Supernatant was discarded and cells were resuspended in 50µl /well Facs buffer containing the antibodies for the surface staining and incubated for at least 35 minutes. 150µl of Facs buffer was added. Cells were spun down at 300g for 2 minutes at 4°C. Supernatant was discarded and cells were

resuspended in 50μl/well Facs buffer containing the Streptavidin antibody to counterstain the biotin antibodies and incubated for at least 15 minutes. 150μl of Facs buffer was added. Cells were spun down at 300g for 2 minutes at 4°C. Supernatant was discarded and cells were resuspended in 100μl/well Fixation kit (eBioscience or BD) to fix the cells and incubated for at least 25 minutes. 100μl of wash buffer (eBioscience or BD) was added. Cells were spun down at 400g for 2 minutes at 4°C. Supernatant was discarded and cells were resuspended in 50μl/well wash buffer (eBioscience or BD) containing antibodies for the intracellular staining and incubated for at least 30 minutes. 150μl of wash buffer (eBioscience or BD) was added. Cells were washed two more times with wash buffer (eBioscience or BD) and acquired on an LSRII (BD Biosciences) flow cytometer (Institute of Immunology, Mainz) or an Celesta (BD Biosciences). Data was analysed using FlowJo software and gating strategies as described in 6.1.1, 6.1.2 and 6.1.3 (Tree Star Inc., BD Biosciences).

Table 2: Antibodies

Antigen	Clone number	Isotype	Fluorochrome	Supplier
CD1d	n.a.	n.a.	PE	Immudex
CD3ξ	145-2C11	Arm. Hamster IgG	Biotin	Biolegend
CD4	GK1.5	Rat IgG2b, κ	BV785, PerCP-ef710, BV605	Biolegend
CD5	53-7.3	Rat IgG2a, κ	Biotin	Biolegend
CD8α	53-6.7	Rat IgG2a, κ	BV711, BV785	Biolegend
CD8α	53-6.7	Rat IgG2a, κ	AF700	eBioscience
CD11b	M1/70	Rat IgG2b, κ	BV711, AF700	Biolegend
CD11c	N418	Arm. Hamster IgG	Pe-Cy7, FITC	Biolegend
CD16/32	93	Rat IgG2a, λ	unconjugated	BioXCell
CD19	6D5	Rat IgG2a, κ	Biotin	Biolegend
CD25	PC61	Rat IgG1, λ	PE, APC	Biolegend
CD45	30-F11	Rat IgG2b, κ	FITC, AF700, BV605	Biolegend
CD90.2	30-H12	Rat IgG2b, κ	BV785, AF700	Biolegend
CD206	MMR	Rat IgG2a, κ	APC	Biolegend
Eomes	Dan11mag	Rat IgG2a, κ	PerCP-ef710, eF660	eBioscience

Eomes	Dan11mag	Rat IgG2a, κ	AF488	Invitrogen
F4/80	BM8	Rat IgG2a, κ	PE	Biolegend
FcξR1a	MAR-1	Arm. Hamster IgG	Biotin	Biolegend
FoxP3	FJK-16s	Rat IgG2a, κ	AF488	eBioscience
Gr1	RB6-8C5	Rat IgG2b, κ	FITC	Biolegend
IFNγ	XMG1.2	Rat IgG1, κ	APC	Biolegend
IFNγ	XMG1.2	Rat IgG1, κ	FITC	eBioscience
IL2	JES6-5H4	Rat IgG2b, κ	PE	Biolegend
IL17A	TC11-18H10.1	Rat IgG1, κ	AF700	Biolegend
Ki67	SolA15	Rat IgG2a, κ	eF450, AF700	eBioscience
Ki67	B56	Rat IgG1, κ	FITC	BD
Ki67	16A8	Rat IgG2a, κ	PE	Biolegend
KLRG1	2F1	Syr. Hamster IgG	PerCP-Cy5.5, BV605, BV421	Biolegend
KLRG1	2F1	Syr. Hamster IgG	FITC	Invitrogen
Ly6C	HK1.4	Rat IgG2c, κ	PerCP-Cy5.5, BV510	Biolegend
MHC-II	M5/114.15.2	Rat IgG2b, κ	BV510, Pacific Blue	Biolegend
NK1.1	PK136	Rat IgG2a, κ	Pe-Cy7, APC, Biotin	Biolegend
PD1	29F.1A12	Rat IgG2b, κ	Pe-Cy7	Biolegend
RORγt	Q31-378	Mouse IgG2a, κ	BV421	BD
Streptavidin	n.a.	n.a.	BV510, BV711	Biolegend
Streptavidin	n.a.	n.a.	V500	BD
TCRβ	H57-597	Arm. Hamster IgG	Biotin	Biolegend
TCRγ/δ	GL3	Arm. Hamster IgG	Biotin	eBioscience
TCRγ/δ	GL3	Arm. Hamster IgG	Pe-Cy7, PE	Biolegend
TNFα	MP6-XT22	Rat IgG1, κ	BV421	Biolegend

5.2.11 Histology and Immunohistochemistry (Yuan et al., 2017)

Liver tissue samples were fixed overnight in 4% paraformaldehyde, embedded in paraffin. Paraffin sections were subjected to hematoxylin-eosin or

immunohistochemistry staining as previously described (Haybaeck et al., 2009). Briefly, paraffin sections (2mm) and frozen sections (5mm) of livers were used for automated staining performed on Bond MAX (Leica) using the DAB detection kit (bornmax). Paraffin-embedded tissue sections were used for staining with 0.1% Sirius red dissolved in saturated picric acid.

5.2.12 Measurement of Serum Parameters (Yuan et al., 2017)

The analysis for ALT and cholesterol was performed with mouse serum on a Roche Modular System (Roche Diagnostics) with a commercially available automated colorimetric system using a Hitachi P-Modul (Roche).

5.2.13 Statistics

Data was analyzed with the help of the Software PRISM, Version 5 or 7 for Mac OS X, GraphPad Software, Inc. As statistical test, t-test was used as indicated. Significance is marked with * ($p<0,05$), ** ($p<0,01$) or *** ($p<0,001$).

5.2.14 Other contributions to this work

CD-HFD experiments were performed at the University Medical Center Mainz and DKFZ Heidelberg with support from [redacted]. [redacted] and [redacted] helped with preparing the livers for flow cytometry and performed H&E, Picrosiriusred and IHC stainings and analyzed ALT and cholesterol levels.

HCHF, CCl_4 and TAA induction was performed by [redacted].

6 Results

6.1 Establishment of methods to analyze the hepatic immune cell compartment

6.1.1 Identification and analysis of hepatic innate lymphoid cells via flow cytometry

To identify subsets of ILCs, first the area of the sideward Scatter (SSC-A) versus the area of the forward scatter (FSC-A) is used to draw a gate on lymphocytes (Figure 4A). In the second plot, the width of the sideward scatter (SSC-W) versus the area of the sideward scatter (SSC-A) are shown (Figure 4B). Thereby, doublets can be excluded from further analysis. Next, another doublet-exclusion step is done by showing the width of the forward scatter (FSC-W) versus FSC-A (Figure 4C). After that, live cells can be identified by gating on live-dead-dye$^-$ cells (Figure 4D). These live cells are further identified as CD45$^+$ lymphocytes (Figure 4E). To exclude myeloid cells that are CD11b$^+$, a next gate is drawn on CD11b$^-$ cells (Figure 4F). Group 1 ILCs are characterized by their NK1.1 expression while not expressing any of the lineage markers (CD3, CD5, CD19, TCRβ, TCRγ/δ and FcξR1a) (Figure 4G). By displaying Eomes versus CD90.2, NK cells are identified by their expression of Eomes while being low to positive for CD90.2 (Figure 4H). ILC1s express CD90.2 but not Eomes. These two subpopulations of ILCs are further characterized by their expression of Ki67, which is a proliferation marker, and CD25, which is the IL2-Ra subunit (Figure 4I and J).

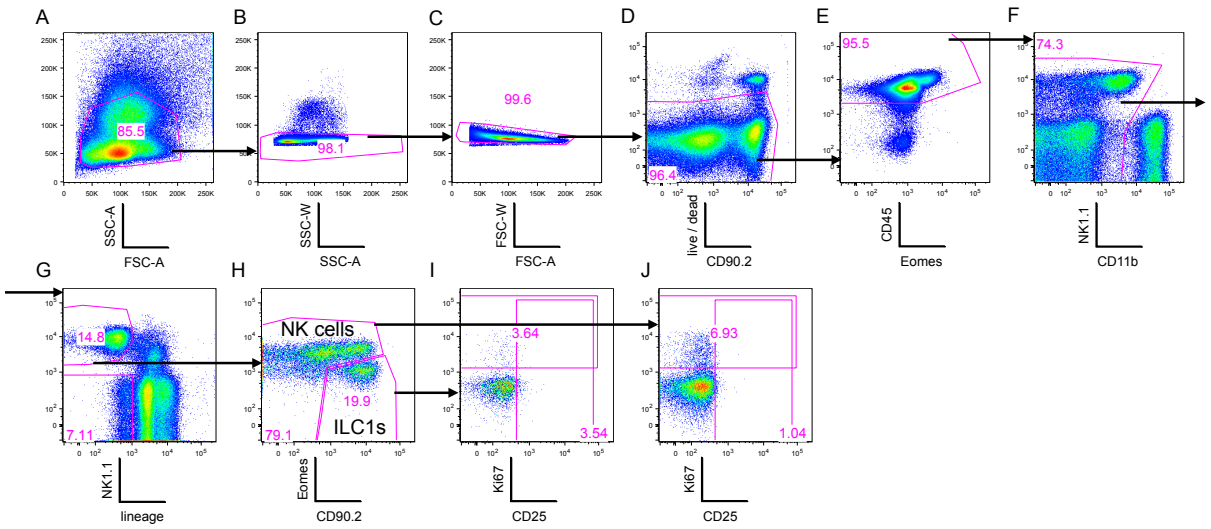

Figure 4: Gating strategy for innate lymphoid cells in the liver

Cell suspensions of livers were stained with viability dye and antibodies against CD90.2, CD45, Eomes, NK1.1, CD11b, lineage (CD3, CD5, CD19, TCRβ, TCRγ/δ, FcξR1a), Ki67 and CD25 and analyzed by flow cytometry. (A) Pre-gating on lymphocytes due to their size and granularity. (B) Exclusion of cell doublets. (C) Another exclusion of cell doublets via FSC-W and FSC-A. (D) Gating on live cells. (E) Gating on CD45^{+} lymphocytes. (F) Group 1 ILCs are gated due to their expression of NK1.1 and negative to intermediate expression of CD11b. (G) Discrimination between NK1.1^{+} lineage^{-} group 1 ILCs and NK1.1^{-} lineage^{-} cells. (H) Differential gating for Eomes^{+} NK cells and CD90.2^{+} Eomes$^{low\text{-}to\ negative}$ ILC1s. (I and J) NK cells and ILC1s can be further investigated due to their expression of Ki67 and CD25 (n=1).

6.1.2 Identification and analysis of hepatic myeloid cells

First, lymphocytes are roughly gated to also include myeloid cells which can appear bigger in the forward-sideward scatter (Figure 5A). Doublet exclusion and definition of live cells is done as described before (Figure 4 and Figure 5B-D). This time, T- (CD3^{+}CD5^{+}), NK- (NK1.1^{+}) and B-cells (CD19^{+}) were excluded (Figure 5E). As a next step, Granulocytes were identified by their high expression of Gr-1 (Figure 5G). Remaining cells were divided into DCs (MHC-II^{+}CD11c^{+}) and non-DCs (MHC-II$^{negative\text{-}to\text{-}low}$ and CD11c$^{negative\text{-}to\text{-}low}$) (Figure 5H). Non-DCs are further gated for their CD11b and F4/80 expression, which marks the MP compartment (Figure 5I). Within this compartment, two major populations can be identified (Figure 5J and K). First, Ly6C^{high} M1-like, rather pro-inflammatory MPs and second Ly6C^{low} MPs that contain CD206^{+} M2-like, rather anti-inflammatory MPs.

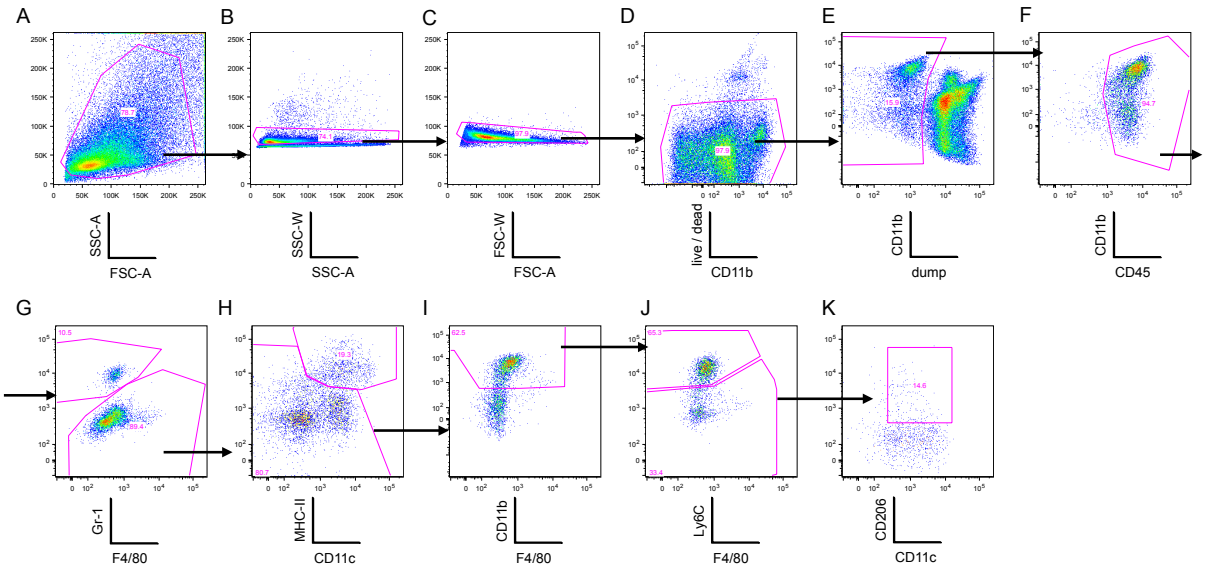

Figure 5: Gating strategy for myeloid cells in the liver

Cell suspension of livers were stained with viability dye and antibodies against CD11b, dump (CD3, CD5, TCRβ, TCRγ/δ, NK1.1), CD45, Gr1, F4/80, MHC-II, CD11c, Ly6C and CD206 and were analyzed by flow cytometry. (A-D) see Figure 4. (E) Exclusion of dump$^+$ cells (T cells, NK cells, B cells stained with CD3, CD5, NK1.1 and CD19 respectively). (F) Gating on lymphocytes. (G) Discrimination of Gr1$^+$ Granulocytes and Gr1$^-$ cells. (H) Discrimination of DCs (MHC-II$^+$CD11c$^+$) and other myeloid cells. (I) Identification of CD11b$^+$F4/80$^+$ MPs. (J) Discrimination between Ly6C^{high} M1-like MPs and Ly6C^{low} MPs. (K) Gating on CD206$^+$ M2-like MPs (n=1).

6.1.3 Identification and analysis of hepatic T cells

The T cell compartment was also characterized by FACS. The first steps were described before (Figure 4 and Figure 6A-D). As soon as living cells are identified, CD4$^+$ T cells are shown and divided into FoxP3$^+$ Tregs and effector T cells (Figure 6F and G). Non-CD4$^+$ T cells are gated as CD8$^+$ T cells (Figure 6I). Tregs and CD3$^+$TCRγδ$^+$ γδ T cells are further characterized by their Ki67 and PD1 expression (Figure 6E and H).

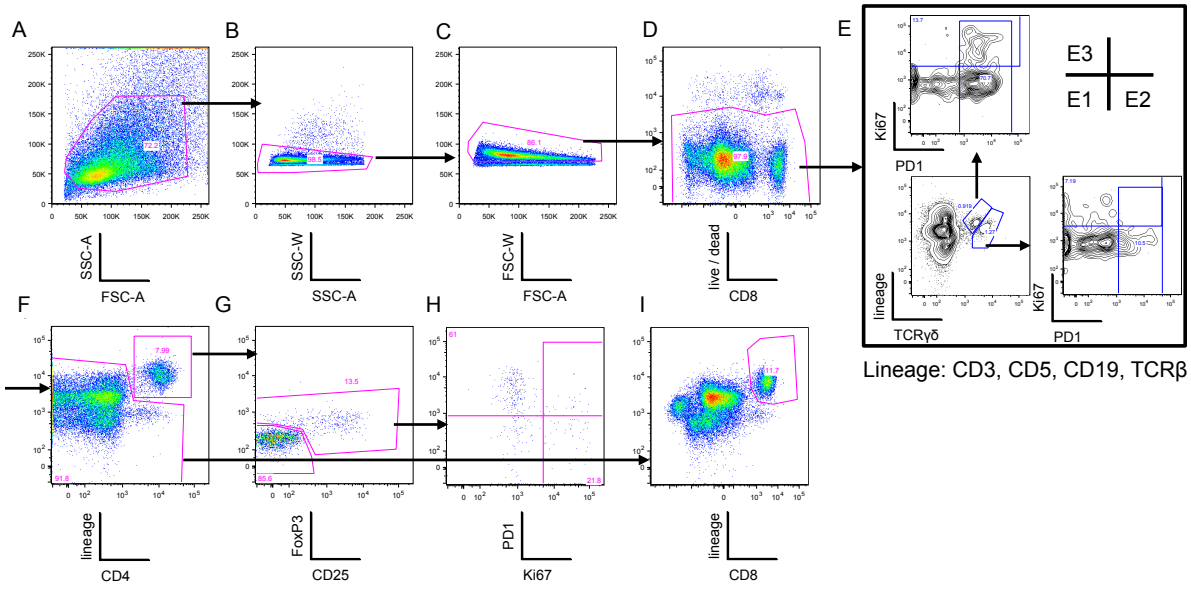

Figure 6: Gating strategy for T cells in the liver

Cell suspension of livers were stained with viability dye and antibodies against CD8, Ki67, PD1, TCRδ, lineage (CD3, CD5, CD19, TCRβ), CD4, FoxP3 and CD25 and were analyzed by flow cytometry. (A-D) see Figure 4. (E) Identification of Vγ4 (TCRγδ^{hi}, Figure 6E2) and Vγ6 (TCRγδ^{int}, Figure 6E3) γδ T cells and their further discrimination by Ki67 and/or PD1 expression. (F) Gating on CD4 T cells and others. (G) Detailed gating of CD4 T cells to divide them into FoxP3^{+}CD25^{+} Tregs and FoxP3^{-}CD25^{-} effector T cells. (H) Subsets of Tregs can be identified by their expression of PD1 and Ki67. (I) Gating on CD8^{+} lineage^{+} CD8 T cells (n=1).

6.2 Splenic ILC1s respond to IL12 and IL18 stimulation with upregulation of CD25 *in vitro*

As the relevance of the IL2 pathway for group 1 ILCs was a major subject of this thesis several tissues were screened for their steady-state CD25 expression on group 1 ILCs (Figure 7). Mesenteric lymph node ILC1s, but not NK cells, readily expressed CD25 *ex vivo* (Figure 7A). NKp46Cre CD25flox mice mesenteric lymph node ILC1s lack the ability to produce CD25. Liver group 1 ILCs, in contrast, did not express CD25 *ex vivo* (Figure 7B). To further test the efficiency of the used conditional mouse model, splenocytes were incubated for 12h with IL2 and left either unstimulated or were stimulated with IL12 and IL18 (Figure 7C and D). IL12 and IL18 stimulation induced a high expression of CD25 on splenic group 1 ILCs. NKp46Cre CD25flox mice-derived splenic group 1 ILCs lacked the ability to express CD25 after *in vitro* stimulation, confirming the efficient deletion of the Il2ra gene in NKp46+ cells (Figure 7D).

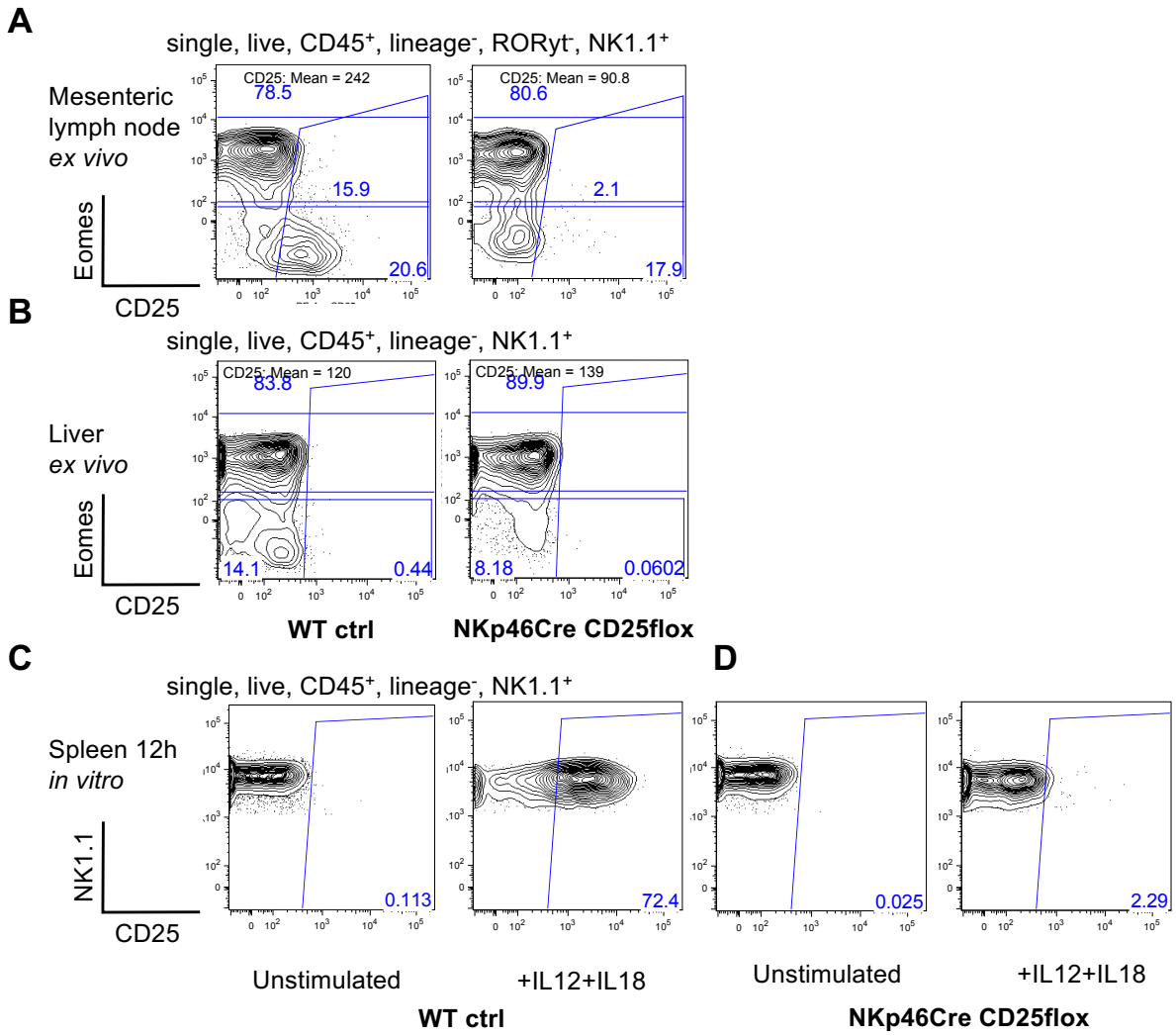

Figure 7: CD25 expression *ex vivo* and after 12h *in vitro* stimulation with IL12 and IL18 in wild type and in NKp46Cre CD25flox mice

Mesenteric lymph nodes (A), the liver (B) and the spleen (C, D) from wild type and NKp46Cre CD25flox mice were analyzed by flow cytometry. Plots show the pre-gated cell population indicated on top of each plot. Target cell populations were gated as Eomes vs. CD25 (A and B) or NK1.1 vs. CD25 (C, D). Gates show the distribution of cells within the plot shown. Gating in (A) differentiates between Eomes$^+$ NK cells (top number), Eomes$^-$ ILC1s (bottom number) and CD25$^+$ (middle number) cells within all group 1 ILCs. Gating in (B) differentiates between Eomes$^+$ NK cells (top number), Eomes$^-$ ILC1s (bottom left number) and CD25$^+$ (bottom right number) cells within all group 1 ILCs. Gating (C and D) shows CD25$^+$ cells within the whole target population. Plots show representative data from one out of three animals/group in one experiment. Lineage = CD3, CD5, CD19, TCRβ, TCRγ/δ.

These analyses of *ex vivo* and *in vitro* expression of CD25 on group 1 ILCs showed that CD25 is expressed in steady state in mesenteric lymph node ILC1s and can be induced in splenic group 1 ILCs by IL12 and IL18 stimulation. The expression and upregulation of CD25 can be manipulated by the use of NKp46Cre CD25flox mice that

lacked the expression of CD25 on group 1 ILCs. This model therefore provides a way to characterize the role of the IL2 pathway in group 1 ILCs.

6.3 ILC1s are affected by CD-HFD and play a role in IL2 signaling to promote HCC

Liver NK cells and ILC1s represent about 5-10% of all lymphocytes in the liver. NK cells are specialized in the clearance of viral infections and killing of transformed cells (Fasbender et al., 2016). In human livers, they resemble around 50% of all lymphocytes and in the mouse around 5-10%. It was previously shown that NK cells and ILC1s can exacerbate the development of obesity-induced chronic inflammation and insulin resistance in adipose tissues (O'Sullivan et al., 2016; Wensveen et al., 2015). Lipid accumulation caused by a high fat diet leads to hepatocyte death in the liver that activates lymphocytes. To study the role of NK cells and ILC1s in the early development of liver fibrosis, NASH and HCC, CD-HFD on C57BL/6 WT mice for 1,5, 3, 6 and 12 months was performed. CD-HFD was previously described to closely resemble the human stages of liver diseases (M. J. Wolf et al., 2014).

Flow cytometry was performed to analyze different cell compartments at the end of the experiments. ALT and cholesterol in the serum of the mice serve as a readout for the progression of the liver disease (Figure 8A and B). Both markers are increased after 3 months on diet and the difference between (CD-) HFD and normal chow diet (NCD) increases over time. The stages of disease can also be characterized with the help of H&E or Picrosirius Red Stain, showing lipid accumulation and collagen deposition, respectively (Figure 8C).

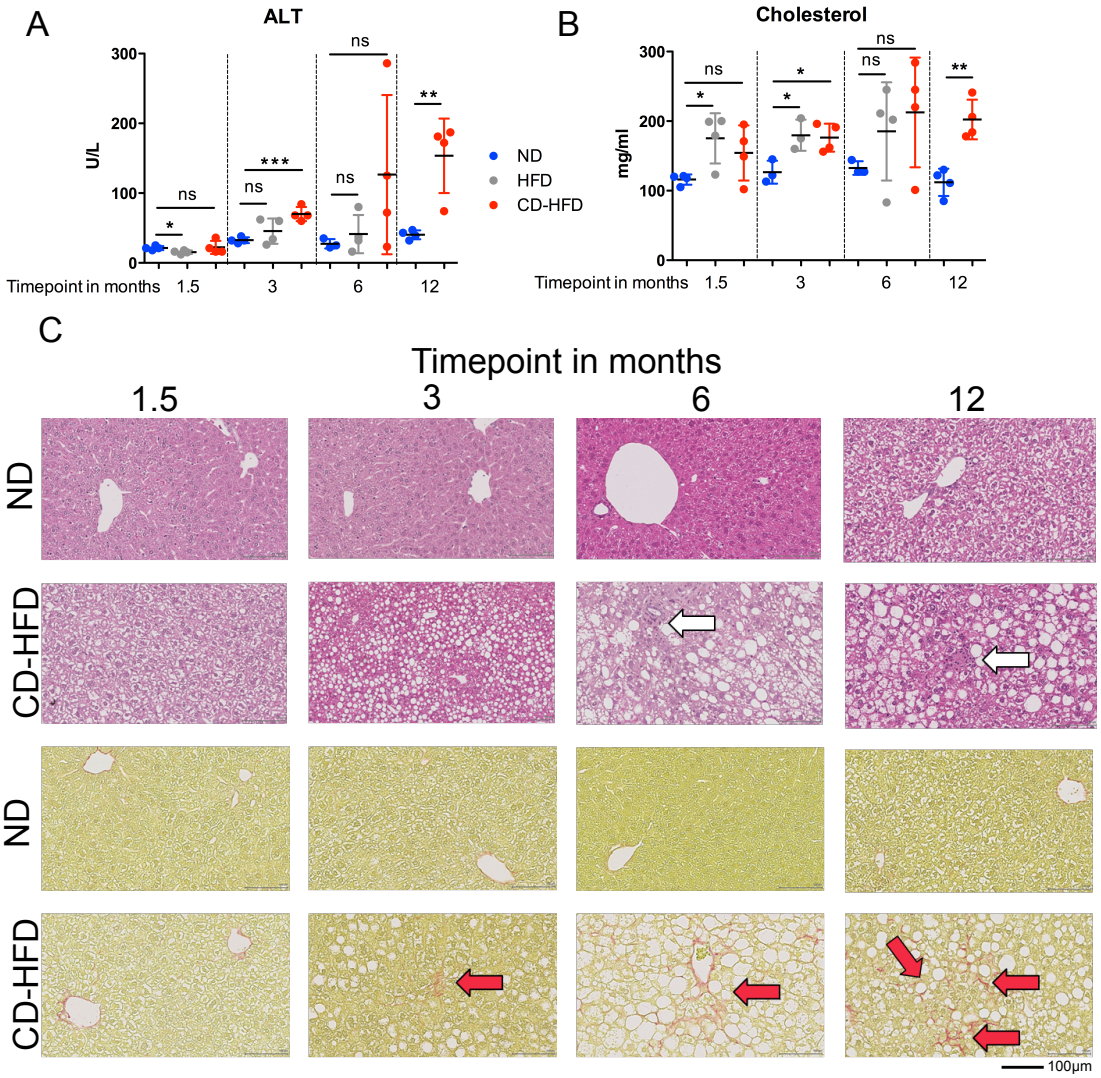

Figure 8: CD-HFD leads to increased liver parameters, lipid accumulation and collagen deposition in the liver

Mice were kept 1,5, 3, 6 or 12 months on normal diet, HFD or CD-HFD. (A) Blood levels of ALT were assessed by collection from the facial vein. Levels are shown in Units/Liter. (B) Blood levels of Cholesterol were assessed by collection from the facial vein. Levels are shown in mg/ml. (C) Liver biopsies were collected and either paraffin-embedded (H&E) or snap-frozen (Picrosirius red stain) to determine immune cell infiltration (H&E, top rows) and collagen deposition (Picrosirius Red stain, bottom rows). White arrows show lipid accumulation (H&E), red arrows show collagen deposition.

NK cells and ILC1s show a higher proliferation rate in HFD and CD-HFD experiments already after 1,5 months (Figure 9A - D). This effect, partly exclusive for the CD-HFD stays consistent over the kinetics up to 12 months. Surprisingly, there are no changes in absolute numbers of NK cells and ILC1s, except the increase in the CD-HFD group after 6 months (Figure 9E - H).

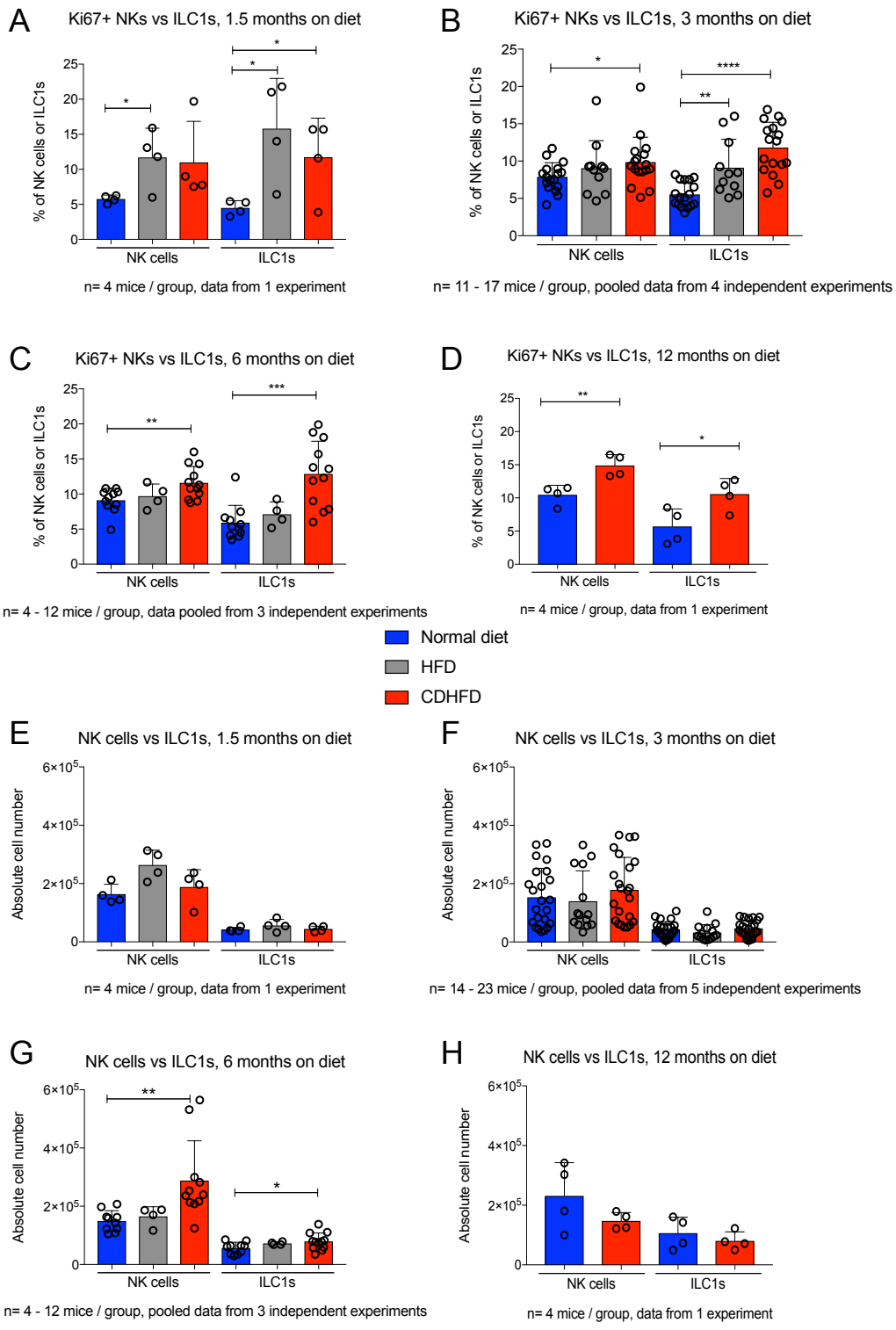

Figure 9: CD-HFD increases proliferation of group 1 ILCs

Mice were kept 1,5 (A and E), 3 (B and F), 6 (C and G) or 12 (D and H) months on normal diet, HFD or CD-HFD. (A - D) Ki67^{+} fraction of NK cells and ILC1s is shown after each of the time points as indicated. (E – H) Quantification of absolute cell numbers were determined with counting beads before Percoll enrichment. Bars show NK cells or ILC1s after the indicated diet. The data are shown in mean ± SEM and display all of one to five experiments (n= 4-23 mice/group). *,P < 0,05; **,P < 0,005; ***,P < 0,0005; ****,P < 0,0001; ns, not significant.

Intracellular staining for cytokine production was performed to study the functional role of Group 1 ILCs (Figure 10). They rather produce less IFNγ (NK cells and ILC1s, Figure 10A and B), TNFα (ILC1s, Figure 10D) and IL2 (ILC1s, Figure 10C) in the CD-HFD mice, especially in the late time points after 1,5 months. Group 1 ILCs might be suppressed in their cytokine production during CD-HFD by other cells or extrinsic factors.

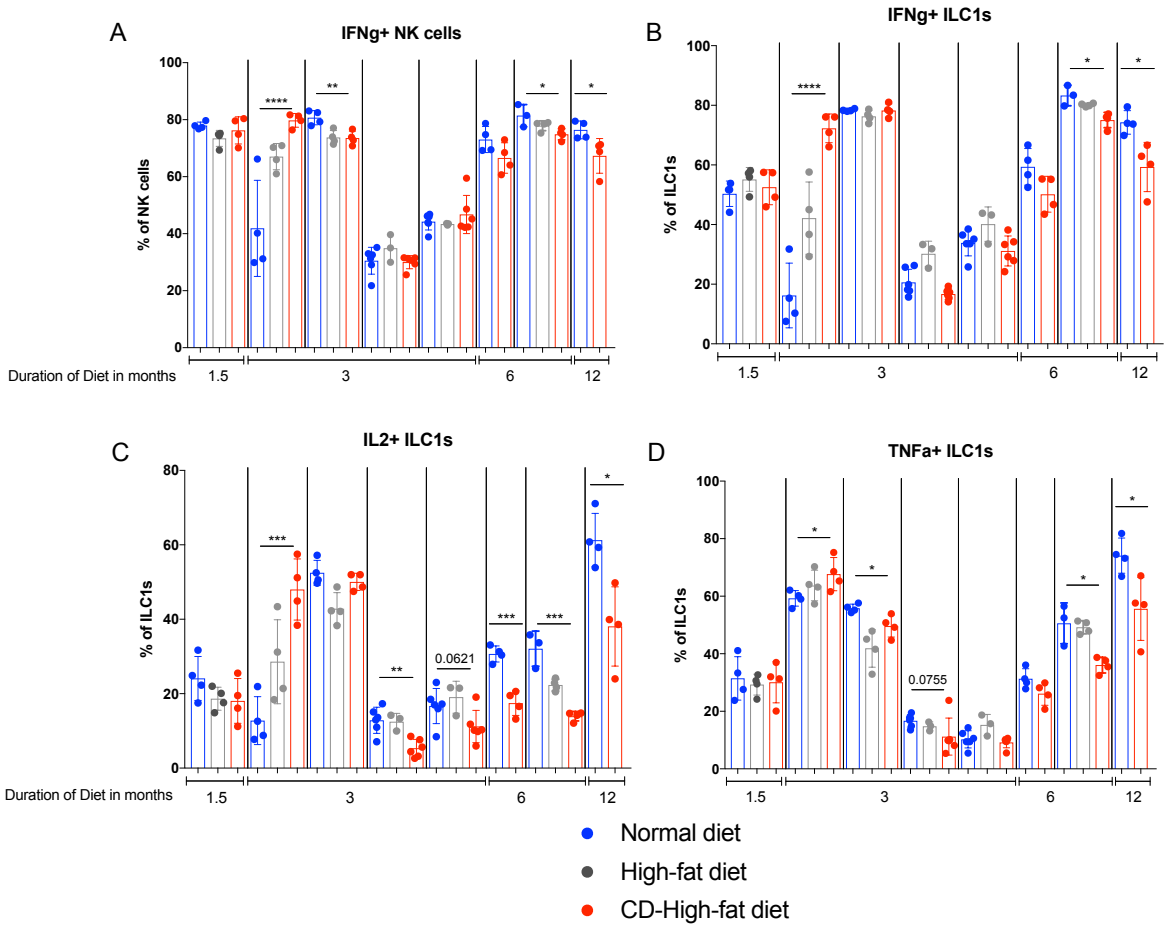

Figure 10: CD-HFD decreases cytokine production of group 1 ILCs

Mice were kept 1,5, 3, 6 or 12 months on normal diet, HFD or CD-HFD. IFNγ (A and B), IL2 (C) and TNFα (D) production was assessed after Percoll enrichment and 4h stimulation at 37°C with Brefeldin A, PMA and Ionomycin. Cytokines were stained intracellular after BD kit fixation and analyzed by flow cytometry. Data show the frequency of IFNγ$^+$, IL2$^+$ or TNFα$^+$ cells within the indicated cell population after the indicated duration of the diet. The data are shown in mean ± SD (n= 3-6 mice/group). *,P < 0,05; **,P < 0,005; ***,P < 0,0005; ****,P < 0,0001; ns, not significant.

Further experiments were performed with mice that lack either all NKp46 expressing cells (NKp46Cre x iDTA) or IL2 production of these cells. As previous experiments

showed the decreased cytokine production especially after 6-12 months and HCC develops starting from 8 months on, mice were analyzed at the 8-month time point. The lack of NKp46^{+} cells or IL2^{+} NKp46^{+} cells were confirmed via FACS (Figure 11A and B). ALT levels were slightly decreased in both KO groups (Figure 11C). Tumor incidence, counted after macroscopic phenotype of the livers was only present in the control groups but not in the KO groups (Figure 11D and E).

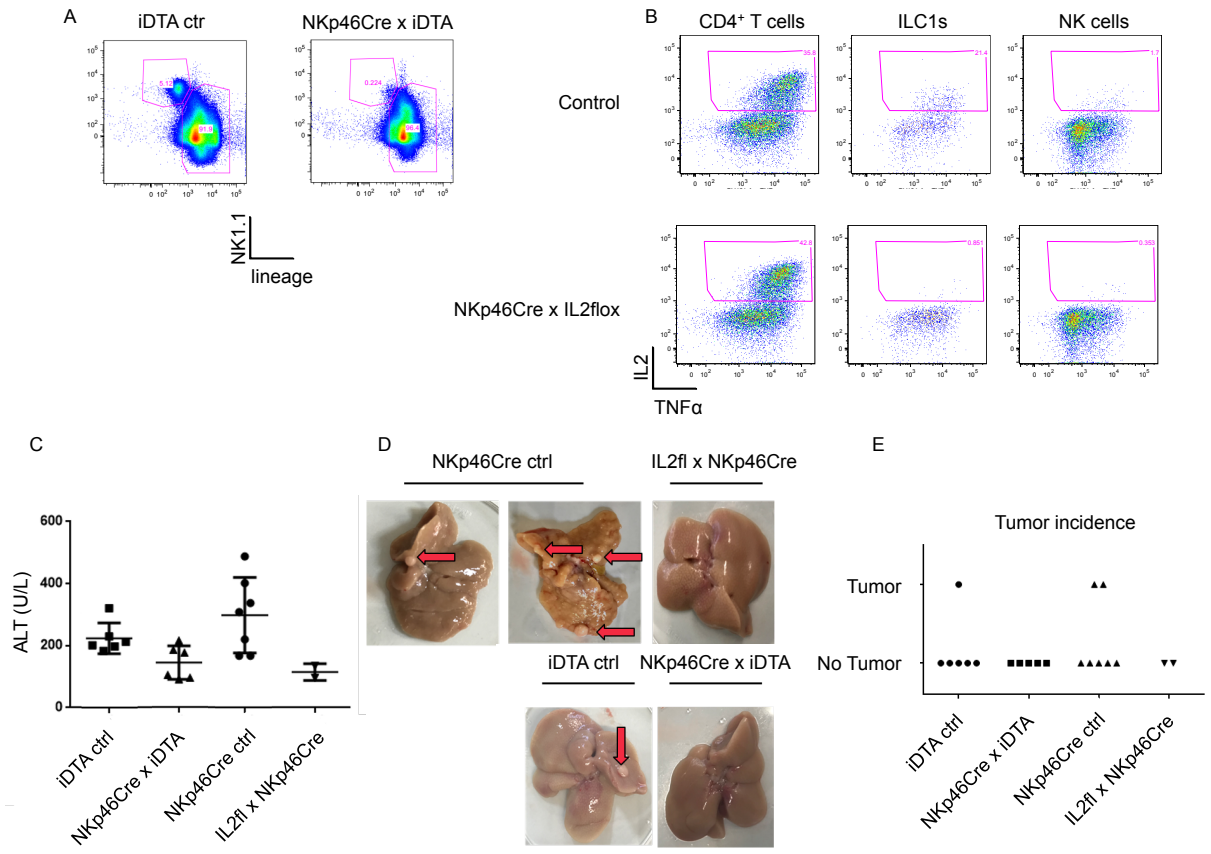

Figure 11: IL2-deficient group 1 ILCs and group 1 ILC-deficient mice show lower tumor incidence after CD-HFD

(A) NKp46Cre x iDTA mice lack group 1 ILCs in the liver. FACS plots show the comparison of WT vs KO mice. Cells were pre-gated on live, CD45^{+} cells. (B) NKp46Cre x IL2fl mice lack IL2 production specifically on NKp46^{+} cells. All plots show cells pre-gated on live, CD45^{+} cells. CD4 T cells are identified as lin^{+}, CD4^{+} cells, ILC1s as lin^{-}, NK1.1^{+}, Eomes low and CD90^{+} cells and NK cells as lin^{-}, NK1.1^{+}, Eomes^{+} cells. Data show representative FACS plots of one or two experiments (n= 2-6 mice /group). (C) ALT values were analyzed from the serum by heart punction after sacrificing the mice. Values show Units/liter. Macroscopic images of livers after perfusion. Red arrows show liver nodules with tumors. Data shows all tumor incidences and representative non-tumor livers. Tumor incidence was counted and livers without nodules counted as non-tumor from one experiment with n= 2-6 mice/group.

This rather milder phenotype was further confirmed with H&E and IHC staining of the liver (Figure 12A and Figure 13A). There were no differences in T cell populations in FACS (Figure 12B and Figure 13B). M2-like MPs are increased in percentage of $F4/80^{+}CD11b^{+}$ or of living cells in the NKp46Cre x iDTA mice (Figure 12C). Tregs were slightly increased in the IL2fl x NKp46 Cre mice and M1-like MPs were slightly higher and M2-like lower in percentage of $F4/80^{+}CD11b^{+}$ MPs (Figure 13B and C).

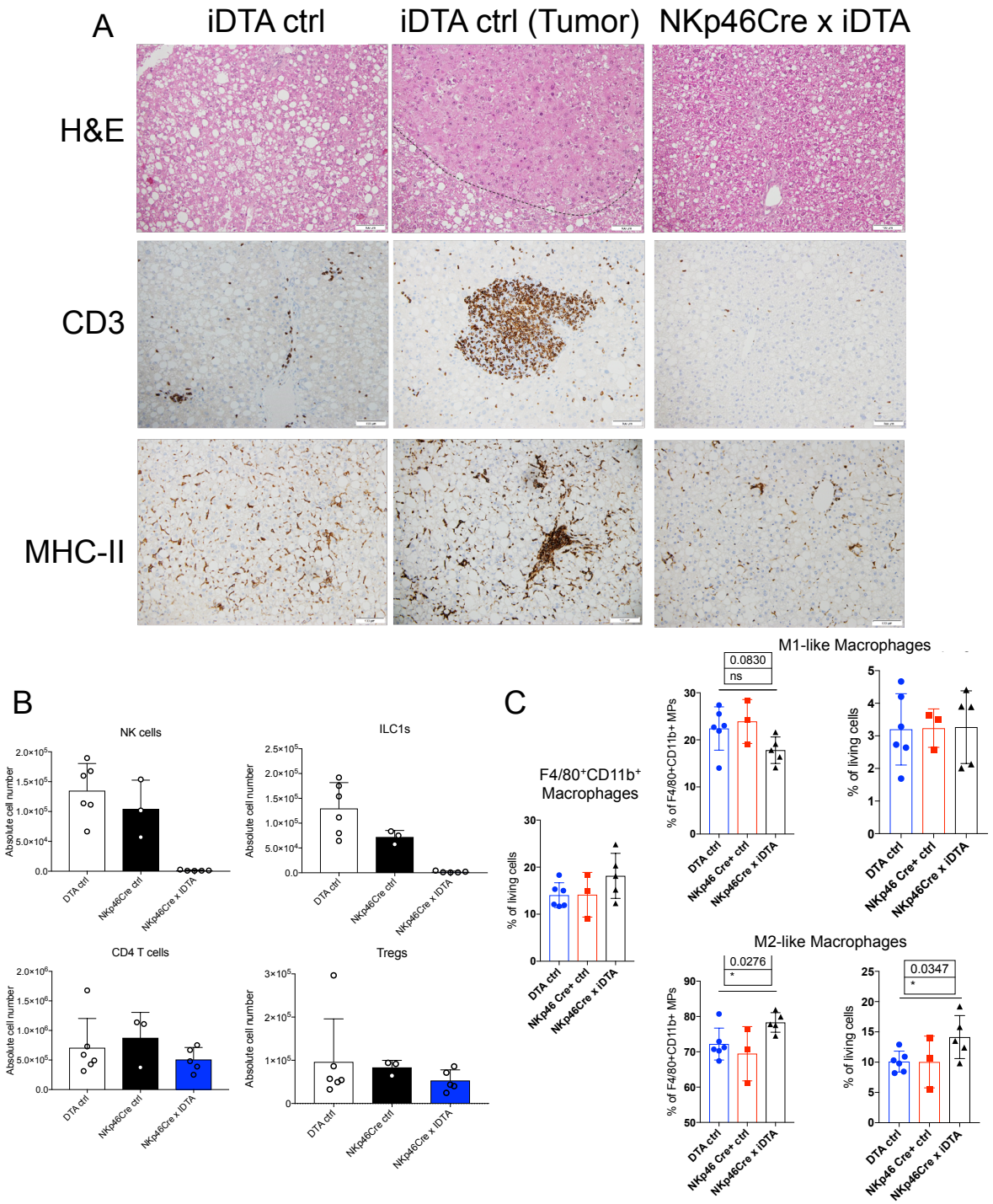

Figure 12: Lack of group 1 ILCs leads to increased M2-like MP frequencies after CD-HFD

(A) Liver biopsies were collected and paraffin-embedded to determine the immune cell infiltration (H&E, top row) and $CD3^+$ or $MHC\text{-}II^+$ cells (IHC, bottom rows). Black bars represent 100µm. (B) Quantification of indicated liver cell populations by FACS as absolute cell number, gated as shown in Figure 6. (C) The myeloid compartment was analyzed by FACS as shown in Figure 5. Data shows representative slides or mean ± SD from one experiment with n= 3-6 mice. *,P < 0,05; **,P < 0,005; ***,P < 0,0005; ns, not significant.

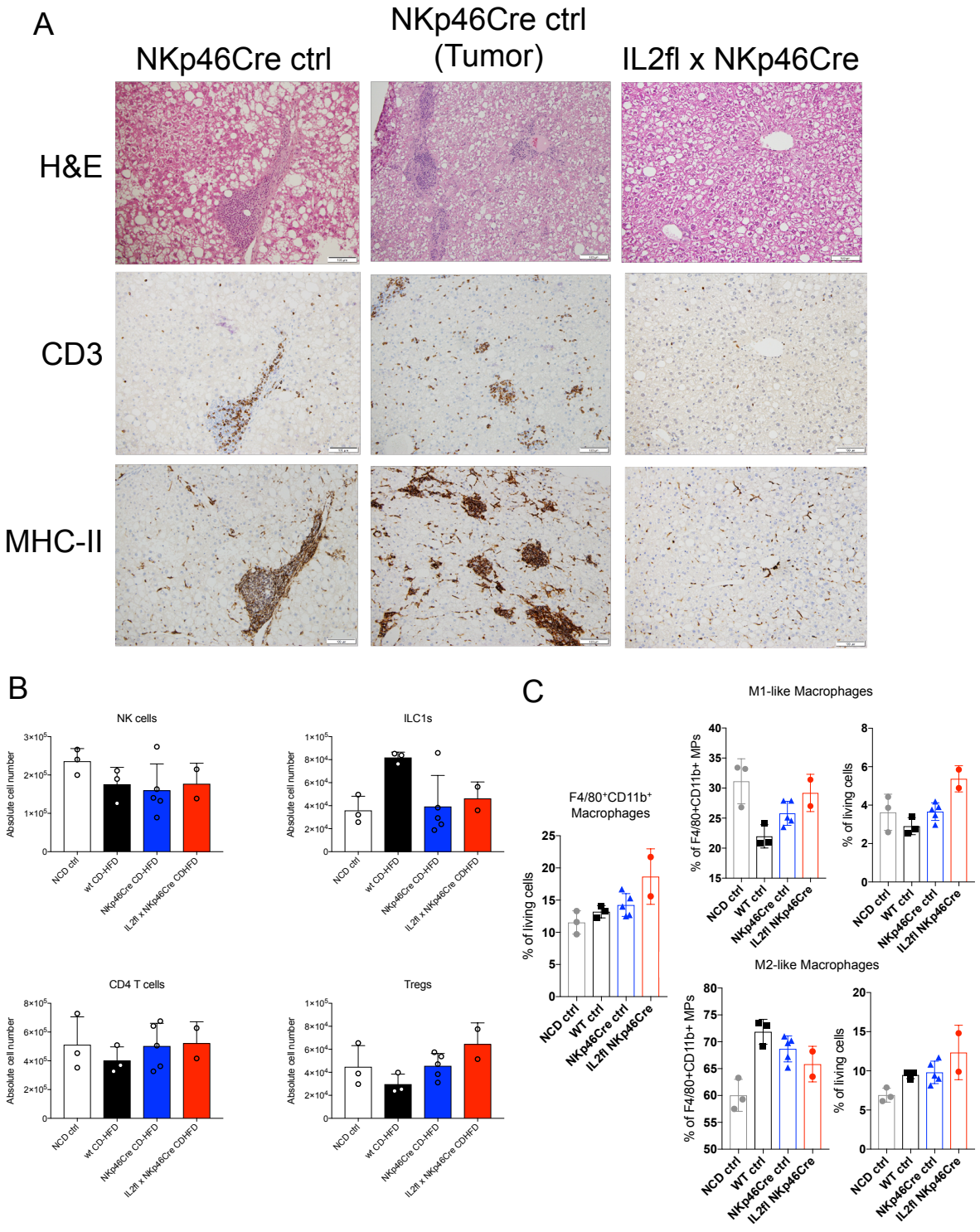

Figure 13: IL2 deficient group 1 ILCs do not significantly change the histopathology and immune cell compartment of the liver after CD-HFD

(A) Liver biopsies were collected and paraffin-embedded to determine the immune cell infiltration (H&E, top row) and CD3$^+$ or MHC-II$^+$ cells (IHC, bottom rows). Black bars represent 100µm. (B) Quantification of indicated liver cell populations by FACS as absolute cell number, gated as shown in Figure 6. (C) The myeloid compartment was analyzed by FACS as shown in Figure 5. Data shows representative slides or mean ± SD from one experiment with n= 3-6 mice. *,P < 0,05; **,P < 0,005; ***,P < 0,0005; ns, not significant.

Unfortunately, a repetition of the experiment with the analysis at the 6 month time point with IL2fl x NKp46Cre mice could not resemble the first observation (data not shown). As a conclusion, especially ILC1s might contribute to the development of NASH and HCC via their IL2 production. The first run with KO mice might hint towards a devastating role for group 1 ILCs and their production of IL2 as the KOs showed a milder phenotype. Further experiments and repetitions need to be performed to clearly identify the role of group 1 ILCs in the development of NASH and HCC.

As high-fat diet was also shown to promote the development of NASH and HCC, additional experiments were done to study the role of group 1 ILCs in this model.

6.4 ILC1s highly upregulate CD25 after high-fat and high-carb diet but not after high-carb diet only

As previously shown, ILCs and NK cells might play a role in the CD-HFD-induced NASH-to-HCC-development. The next step was to investigate if these cells might also be food-derived nutrient-dependent. Fat gets absorbed from the food and is mainly stored as lipids in the different adipose tissues of the body. These lipids can relocate and accumulate in the liver. HC and HFHC experiments were performed to investigate the role of lymphocytes in the early development of NASH and the specific contribution of high fat (10% fat) and high carb content. Additionally, to the shown data from flow cytometry a glucose tolerance test, analysis of different inflammatory marker by qPCR and analysis of serum parameters for liver damage were performed but showed no major differences (data not shown). Flow cytometry shows that ILC1s decrease slightly in percentage of NK1.1^{+} or living cells after 8 and 12 weeks (Figure 14A and D). At the same time, the expanded cells expressed more CD25 and partly more Ki67 (Figure 14B-C and E-F). These results point towards a role of CD25^{+} ILC1s in the development of NASH/NAFLD. At the same time, the effects seem to be fat-dependent as mainly the high-fat diet group showed increased proliferation and CD25 expression.

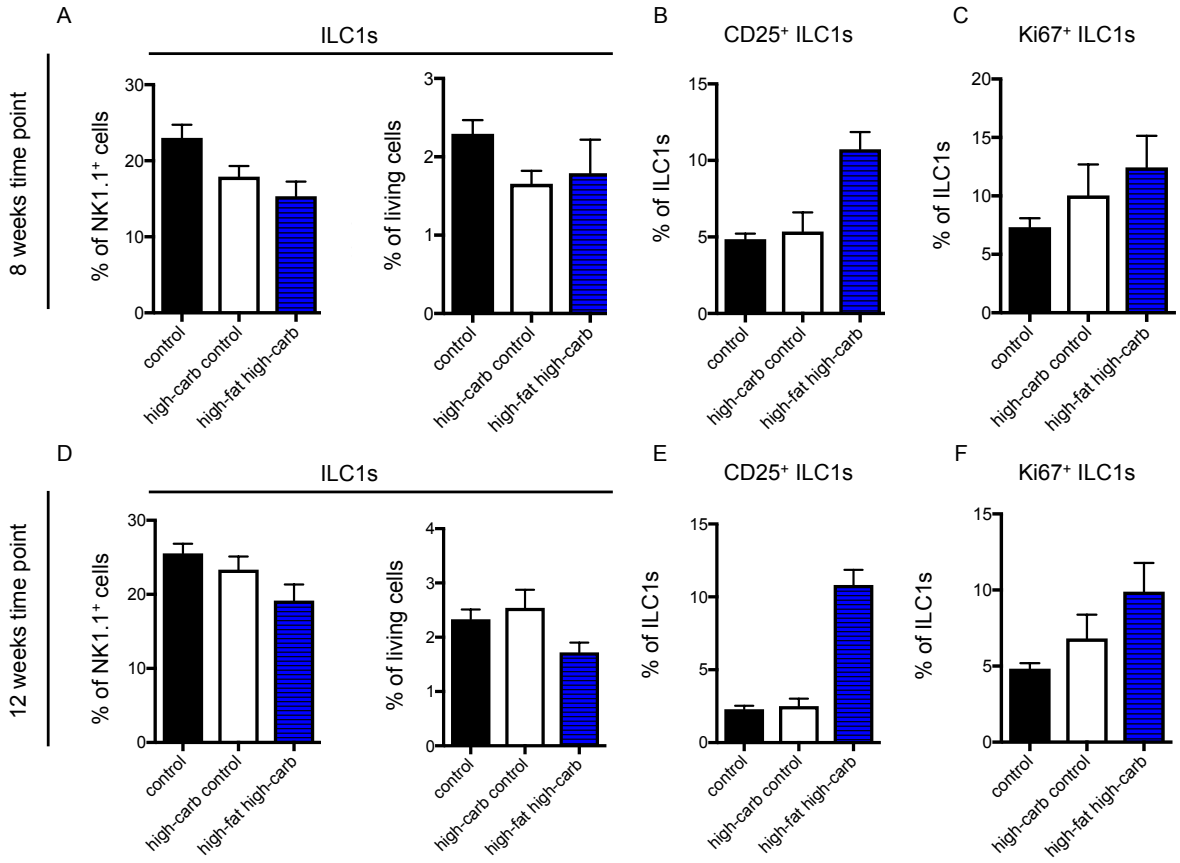

Figure 14: ILC1s upregulate CD25 after high-fat and high-carb diet

Mice were fed a high-fat diet or a normal chow diet. The drinking water was substituted with sucrose or not. Liver ILC1s were analyzed by FACS. Cells were identified as described earlier (Figure 4). ILC1s are displayed in frequency of NK1.1$^+$ cells or of living cells. Of all ILC1s, CD25$^+$ and Ki67$^+$ are shown separately as frequency of all ILC1s. Data show mean ± SEM from one experiment per time point with n= 5-10 mice/group.

6.5 CCl_4-induced liver fibrosis leads to activation of the myeloid and Treg compartment and to high upregulation of CD25 on ILC1s

The previous results hint towards a role of group 1 ILCs and especially the ILC1s in the development of NAFLD. The model of CCl_4-induced liver fibrosis was chosen to further study their role in liver diseases. The advantage of the diet-induced NAFLD models is their close proximity to the human disease. However, the major drawback is the time-consuming assay for the late time points. Therefore, the long known hepatotoxicity of CCl_4 and thereby well-established model of CCl_4-induced liver fibrosis was used to induce liver fibrosis after a relatively short treatment of several weeks (Popov et al., 2011; Williams et al., 1990).

To identify the potentially different roles of group 1 ILCs in the progression and the reversal phase, CCl_4-induced fibrosis experiments were performed with C57BL/6 WT mice. Therefore, the cell subsets in the liver were analyzed after 3 weeks of induction or after 3 weeks of induction plus 1 week of recovery without CCl_4 treatment. $Gr1^+$ and $CD11b^+$ cells increase significantly in the progression but are back to the level of the untreated group in the regression phase (Figure 15A and B). Pro-inflammatory MPs are elevated in the progression phase whereas anti-inflammatory MPs expand in the reversal phase to contribute to tissue healing (Figure 15C and D). Regulatory T cells massively expand during the acute, inflammatory phase of the induced fibrosis and go back to control levels in the reversal phase (Figure 15E-G). ILC1s are differentially involved in the stages of disease. First, they upregulate CD25 in the progression phase and expand in percentage of living and $NK1.1^+$ cells in the reversal phase (Figure 15I and J). This differential role of ILC1s seems to be cell-specific as NK cells do not show these effects and express rather low amounts of CD25 (Figure 15K, L and data not shown). The specific CD25 expression can enhance the ability of ILC1s to signal for IL2 and support the proliferation and survival (Figure 15M). These results point towards a role of ILC1s in the acute and inflammatory state and in the recovery, tissue-healing phase of CCl_4-induced liver fibrosis. Further studies need to be done on the exact function of CD25 on these cells.

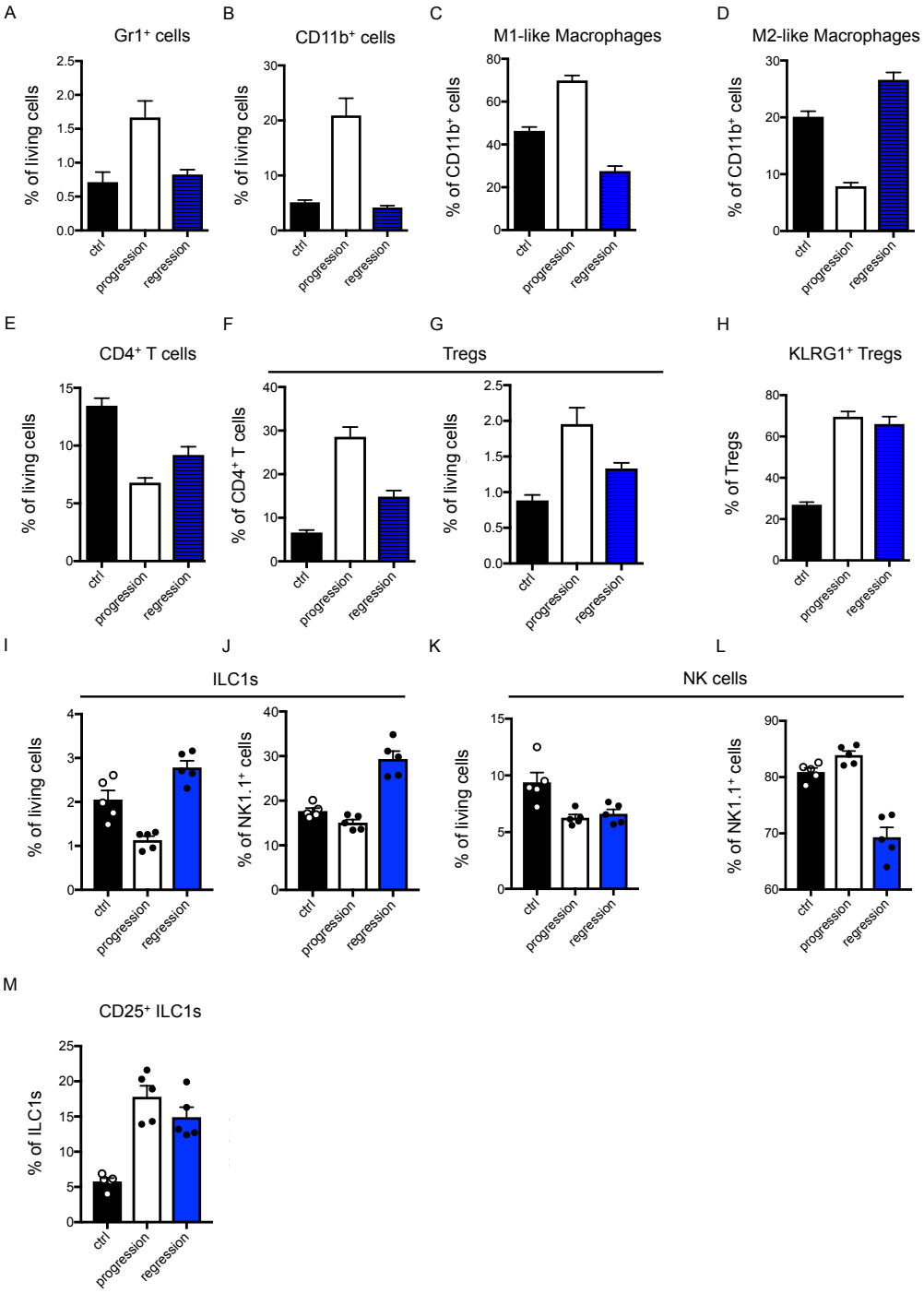

Figure 15: Immune cell compartments change during CCl_4-induced liver fibrosis

CCl_4 was administered by oral gavage 3 times per week in escalating doses. Livers of the mice were analyzed (progression group) or left untreated for 1 week before analysis (regression) by FACS. (A-D) The myeloid cell compartment. (E-H) The T cell compartment. (I-L) The group 1 ILC compartment. (M) CD25 of ILC1s during progression and regression. Cell populations were identified as described previously (Figure 4, Figure 5 and Figure 6) and shown as frequency of living cells or as frequency of the indicated cell population. Data shows mean ± SEM from two independent experiments (n= 5 mice/group).

6.6 MMP3 or MMP8 KO leads to altered immune cell compartments during progression and regression of CCl_4-induced or TAA-induced liver fibrosis

The previous results showed that ILC1s might play a role in the development of CCl_4-induced liver fibrosis. A key feature of liver fibrosis is the excess production of extracellular matrix, which is generated mainly by matrix metalloproteases. They were reported before to contribute to tissue damage during liver fibrosis (de Meijer et al., 2010). The models of CCl_4-induced or TAA-induced liver fibrosis were performed. Mice were analyzed on the acute, progressive phase after 6 weeks or in the reversal phase after 6 weeks induction plus 3 weeks of no treatment. Two candidates of MMPs were investigated for their contribution to liver fibrosis, namely MMP3 and MMP8. A broad analysis of liver lymphocyte populations was done as follows. Additionally to the readout from flow cytometry, collagen content was analysed by Hydroxyproline and Picrosirius Red stain, qRT-PCR was performed for Procollagen a1, α-SMA, TIMP-1, TGFß1, MMP13, MMP9, MMP2, IFNγ, CD68, iNOS, MCP-1, IL10 and serum parameter of ALT, AST, ALP, GGT, LDH, Creatinine, Bilirubin were analyzed but show no major differences (data not shown).

For a general idea of ILC1s in the model of CCl_4, they are shown as percentage of total $CD45^+$ or $NK1.1^+$ cells (Figure 16 A and B). ILC1s slightly increase in the MMP3 KOs in the reversal phase as percentage of $CD45^+$ cells, which is also resembled in the higher fraction of $Ki67^+$ cells (Figure 16A and C). CD25 on ILC1s is differentially regulated and is lower in the MMP3 KOs in the progression phase while being higher in the reversal phase (Figure 16D). The general upregulation of Ki67 and CD25 in the progression is specific for this model as these differences are not present in the TAA model (data not shown). This effect is specific for MMP3KO mice as there are no differences in the MMP8KOs, both in the TAA and CCl_4 model. A general observation is that ILC1s are always expanding in the reversal phase, but not in the TAA MMP8KO experiment (data not shown). As a result, ILC1s might play a role in the reversal phase, especially of CCl_4- but also TAA-induced liver fibrosis and this could be MMP3-mediated. Furthermore, CD25 expression on ILC1s during the progression phase of fibrosis could be important for the development of the disease as it could regulate the IL2 availability. To investigate the role of MMP3 and MMP8 in myeloid cells in the progression and reversal of TAA- or CCl_4-induced fibrosis they are identified by FACS as described before (Figure 16E-H). In the CCl_4 model, MMP3KOs have decreased pro-inflammatory MPs in the reversal phase and increased anti-inflammatory MPs. The

same trend can be seen in the TAA model (Figure 16F and H). This shift in MP populations seems to be MMP3KO-specific as no differences are observed in the MMP8 KOs (data not shown). MPs are involved in fibrosis development. The increase of CD11b$^+$ cells in the progression and the F4/80$^+$ Ly6C^{low} cells in the reversal phase in the TAA- but not in the CCl_4-model points to a model-dependent role and the individual stages of the disease.

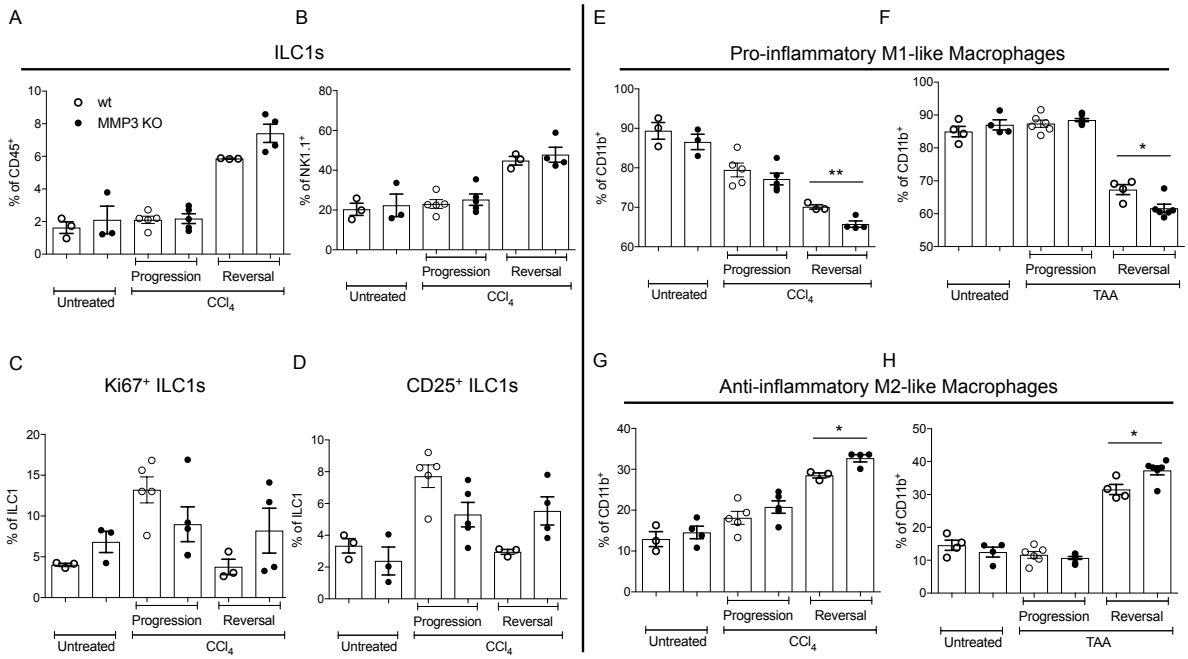

Figure 16: ILC1s and MPs of MMP3KO mice during progression and reversal of CCl_4- and TAA-induced liver fibrosis

MMP3 KO mice or WT mice were treated with CCl_4 or TAA as described previously. Mice were analyzed untreated, at the acute progression phase or at the reversal phase. Livers were prepared as described and cell populations were analyzed by FACS. (A-D) Frequencies of ILC1s are shown as percentage of CD45$^+$ cells or NK1.1$^+$ cells. Ki67 and CD25 expression is shown as frequency of all ILC1s. (E-H) Frequencies of myeloid cells are shown as frequency of CD11b$^+$ cells. Data is shown in mean ± SEM from one experiment with n= 3-6 mice/group. *,P < 0,05; **,P < 0,005; ***,P < 0,0005; ns, not significant.

The quantification of T cells shows higher CD4 T cell and Treg frequencies in the progression phase in the MMP3KOs during CCl_4-induced liver fibrosis (Figure 17A-C). CD4 T cells are reduced in the reversal phase in the MMP3 KO group (Figure 17A). CD8 T cells and γδ T cells are not altered in the MMP3KO mice (data not shown). Nevertheless, there is a tremendous increase in PD1 expression on Vγ6 γδ T cells during progression, which seems to be CCl_4-dependent as these differences are not observed in the TAA model (Figure 17D and E).

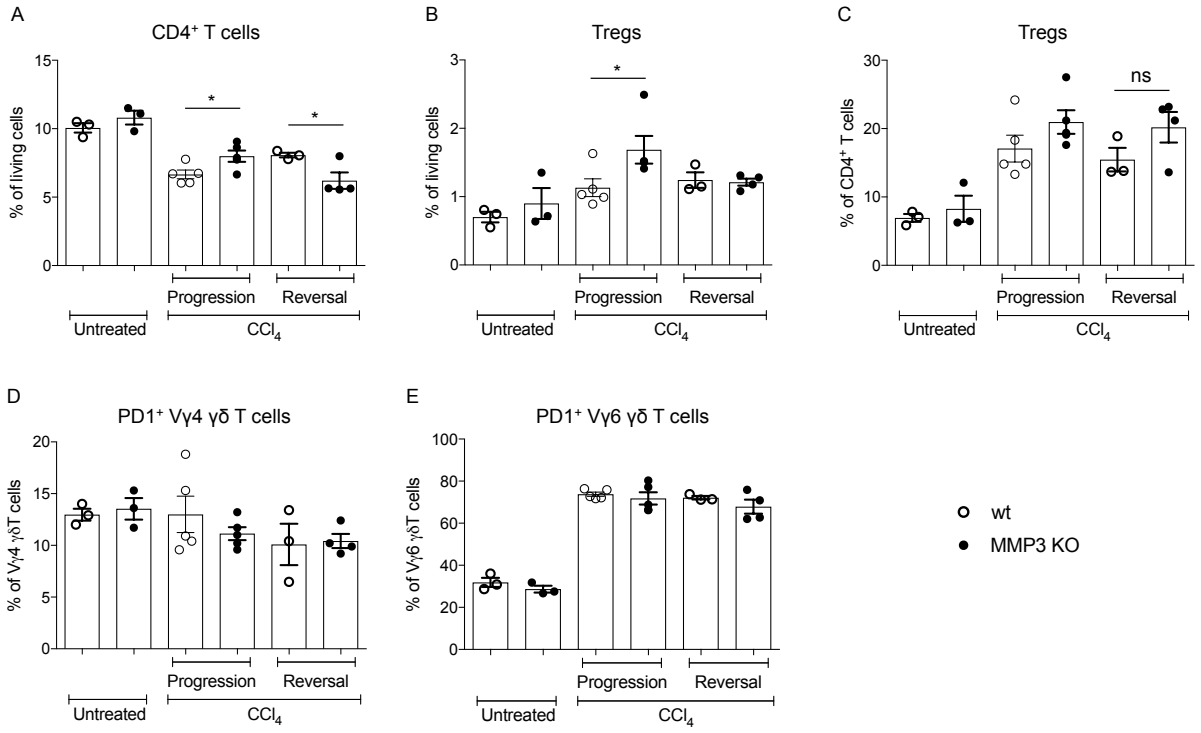

Figure 17: T cell compartment of MMP3KO mice during progression and reversal of CCl_4-induced liver fibrosis

MMP3 KO mice or WT mice were treated with CCl_4 as described previously. Mice were analyzed untreated, at the acute progression phase or at the reversal phase. Livers were prepared as described and cell populations were analyzed by FACS. (A-C) CD4 T cell compartment as percentage of living cells (A), Tregs as percentage of living cells (B) or of CD4 T cells (C). (D and E) γδ T cell compartment as percentage of Vγ4 γδ T cells (D) or Vγ6 γδ T cells (E). Data is shown in mean ± SEM from one experiment with n= 3-5 mice/group. *,P < 0,05; **,P < 0,005; ***,P < 0,0005; ns, not significant

Tregs are highly increased, both in percentage of living-and of CD4 T cells, in the reversal phase of CCl_4-induced fibrosis in the MMP8KOs (Figure 18A-C). In parallel, Tregs show less proliferation and more PD1-expression in this phase (Figure 18D and E). Slightly more Tregs are also present during the reversal phase of TAA-induced fibrosis in the MMP8KOs (Figure 18F and G).

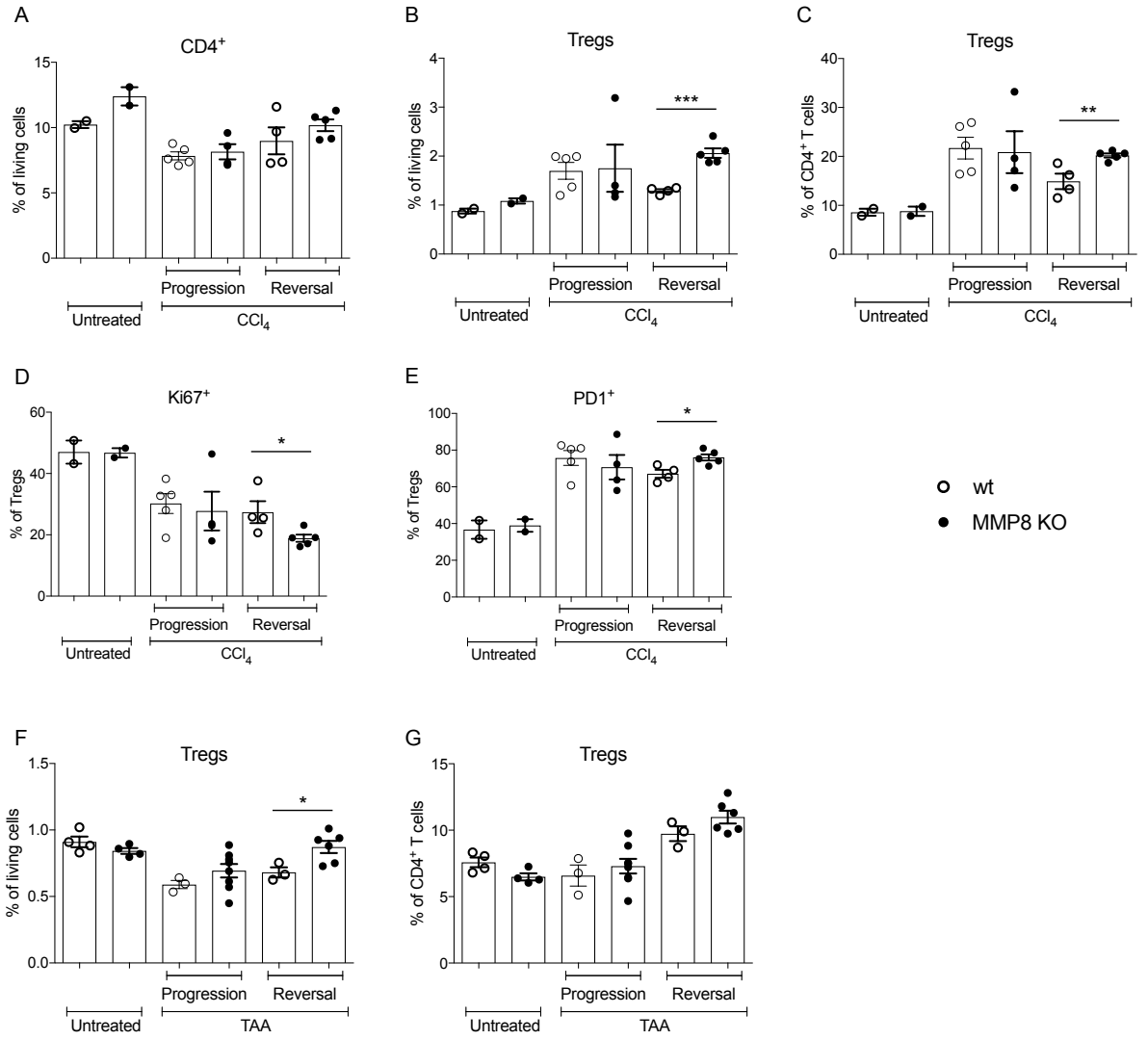

Figure 18: T cell compartment of MMP8KO mice during CCl_4- and TAA-induced liver fibrosis

MMP8 KO mice or WT mice were treated with CCl_4 or TAA as described previously. Mice were analyzed untreated, at the acute progression phase or at the reversal phase. Livers were prepared as described and cell populations were analyzed by FACS.

(A-C) CD4 T cell compartment as percentage of living cells (A), Tregs as percentage of living cells (B) or of CD4 T cells (C) during CCl_4. (D and E) Ki67 (D) and PD1 expression (E) of Tregs. (F and G) Tregs during TAA as percentage of living cells (F) or CD4 T cells (G). Data is shown in mean ± SEM from one experiment with n= 2-7 mice/group. No statistical differences were observed between relevant groups unless indicated as: *,$P < 0,05$; **,$P < 0,005$; ***,$P < 0,0005$.

T cells, especially FoxP3$^+$ Tregs, seem to be involved in the progression and reversal phase of fibrosis and this might partially be mediated by MMP3 or MMP8. This could point to a dual function of these cells in the liver.

6.7 Deletion of CD25 on NKp46$^+$ cells leads to cell-intrinsic and cell-extrinsic effects on innate and adaptive lymphocytes

To further study the role of ILC1s in liver fibrosis after the observation of the upregulation of CD25 on ILC1s in CCl_4-induced fibrosis (Figure 15M), the idea was to perform the experiment with CD25fl x NKp46Cre mice. These mice lack the IL2Rα subunit specifically on NKp46$^+$ cells, which include ILC1s. The first experiment was done to check the role in the early development of fibrosis after 3 weeks of induction (Figure 19). CD4$^+$ T cells, Tregs and CD8$^+$ T cells were slightly increased in CD25fl x NKp46Cre mice as percentage of living cells (Figure 19A-C). CD4 T cells have reduced IL17A production after PMA, Ionomycin and Brefeldin A treatment *in vitro* in percentage of CD4$^+$ T cells (Figure 19D). The ILC compartment was not further altered than the reduced frequencies of group 1 ILCs and the lack of CD25 in NK cells and ILC1s (Figure 19E and F). The reduced number in ILC1s was reported before as an effect of the Cre itself (Narni-Mancinelli et al., 2011).

Interestingly, ILC1s express way more CD25 than NK cells (Figure 19E and F). There was a slight increase in IL2-producing ILC1s lacking CD25 compared to the WT control (Figure 19G). CD25fl x NKp46Cre mice also showed decreased frequencies in total F4/80$^+$ MPs in percentage of living cells (Figure 19H). Gr-1$^+$ Granulocytes are reduced in Cre$^+$ mice (Figure 19I).

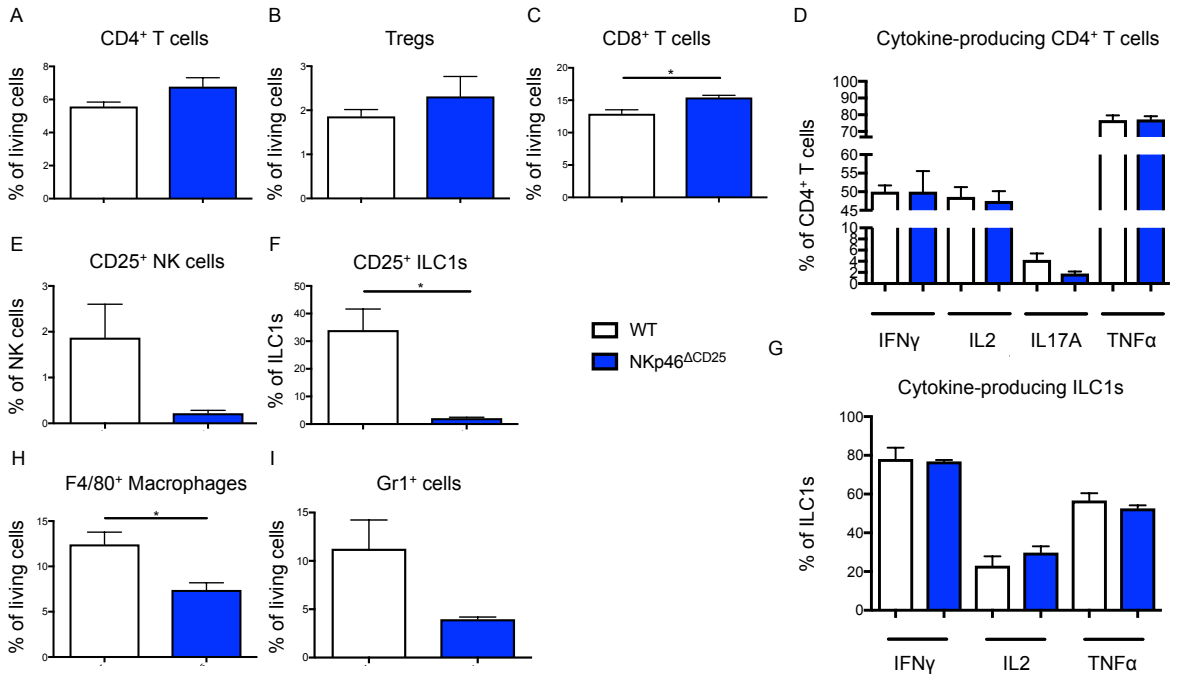

Figure 19: T cell and ILC compartments during CCl_4-induced liver fibrosis in NKp46Cre x CD25flox mice

Mice were treated with CCl_4 by oral gavage 3 times per week for 3 weeks as described before. Single cell suspensions from the liver were analyzed by flow cytometry. (A-C) T cell compartment shown as percentage of living cells. (D) Indicated cytokine production of CD4 T cells as frequency of all CD4 T cells. (E and F) $CD25^+$ cells within the indicated cell compartment. (G) Indicated cytokine production of ILC1s as frequency of all ILC1s. (H) Percentage of MPs within all living cells. (I) Percentage of $Gr1^+$ cells within all living cells. Data is shown in mean ± SEM from one experiment with n= 3 mice/group. No statistical differences were observed unless indicated as: *,P < 0,05; **,P < 0,005; ***,P < 0,0005.

As differences were shown in the first experiment at the early time point of 3 weeks, the next step was to also check for the later time point of 6 weeks to further investigate a role of CD25 on ILC1s. This time, untreated controls were included as well. CD25 was highly upregulated after CCl_4 treatment with an increase from about 2% to up to one third of all ILC1s expressing it (Figure 20A and B). NK cells, when compared to ILC1s, express very low levels of CD25 (Figure 20C). At the same time, more ILC1s were $IL2^+$ in the KO mice in all three experiments (Figure 20D). Another interesting point is the downregulation of IL2 during CCl_4-induced liver fibrosis. CD4 T cells were slightly decreased and Tregs increased in Cre^+ mice whereas CD8 T cells showed no major differences (Figure 20E, F and data not shown). There were no changes in the MP compartment (data not shown). Additionally to the shown data from flow cytometry, different inflammatory markers were analyzed by qPCR, serum parameter were

analyzed to track liver damage and liver pathology was imaged by Picrosirius red and H&E stain but showed no major differences (data not shown).

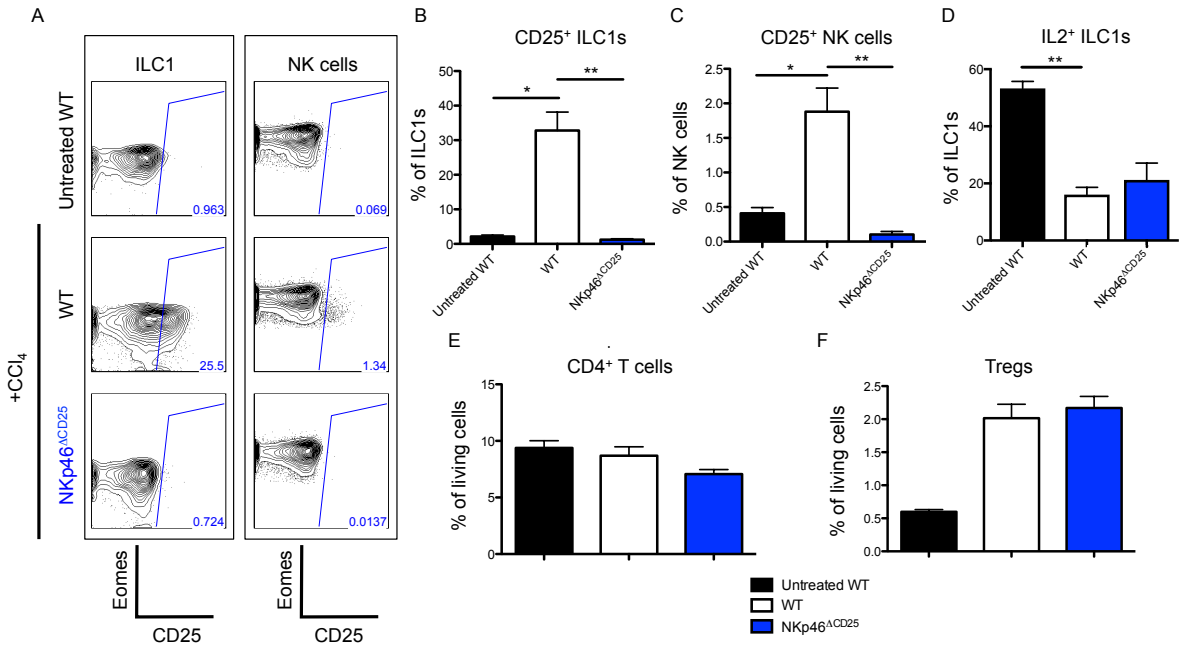

Figure 20: ILC1s upregulate CD25 after CCl_4-induced liver fibrosis

Mice were treated with CCl_4 for 6 weeks as described before. Single cell suspensions from the liver were analyzed by flow cytometry. (A) Representative FACS plots are shown to illustrate CD25 expression on ILC1s and NK cells. (B and C) Quantification of frequencies of $CD25^+$ cells within ILC1s and NK cells. (D) $IL2^+$ cells within the ILC1 compartment. Cytokine production of group 1 ILCs was analyzed after 4h stimulation with Brefeldin A, PMA and Ionomycin at 37°C. (E) CD4 and (F) Tregs as percentage of living cells. Data is shown in mean ± SEM from one experiment with n= 2-3 mice/group. No statistical differences were observed between relevant groups unless indicated as: *,P < 0,05; **,P < 0,005; ***,P < 0,0005.

To figure out a possible role on the reversal phase of fibrosis a 6 week induction plus 3 weeks reversal experiment was performed. This time, 4 untreated mice and 6 NKp46Cre x WT mice were used as controls.

CD4 T cells and Tregs were slightly increased in Cre^+ mice as percentage of living cells and also had a slightly reduced production of IL2 in percentage of all CD4 T cells (Figure 21A, B and D). CD8 T cells are not affected (Figure 21C). NK cell and ILC1 compartment was not affected further than the previously mentioned effect of reduced numbers in $NKp46Cre^+$ mice (Figure 21E-H). CD25-deficient ILC1s express, like in the experiments during the acute phase (Figure 20D), more IL2 than control ILC1s (Figure 21I). The cytokines IFNγ and TNFα were also analyzed but do not show differences

between NKp46Cre ctrl and NKp46Cre CD25flox groups. The results point to a cell-intrinsic role for CD25 on ILC1s, especially by regulating the IL2 production and a potential cell-extrinsic effect on the IL2 production of CD4 T cells. This might be important for the general IL2 availability in fibrotic livers.

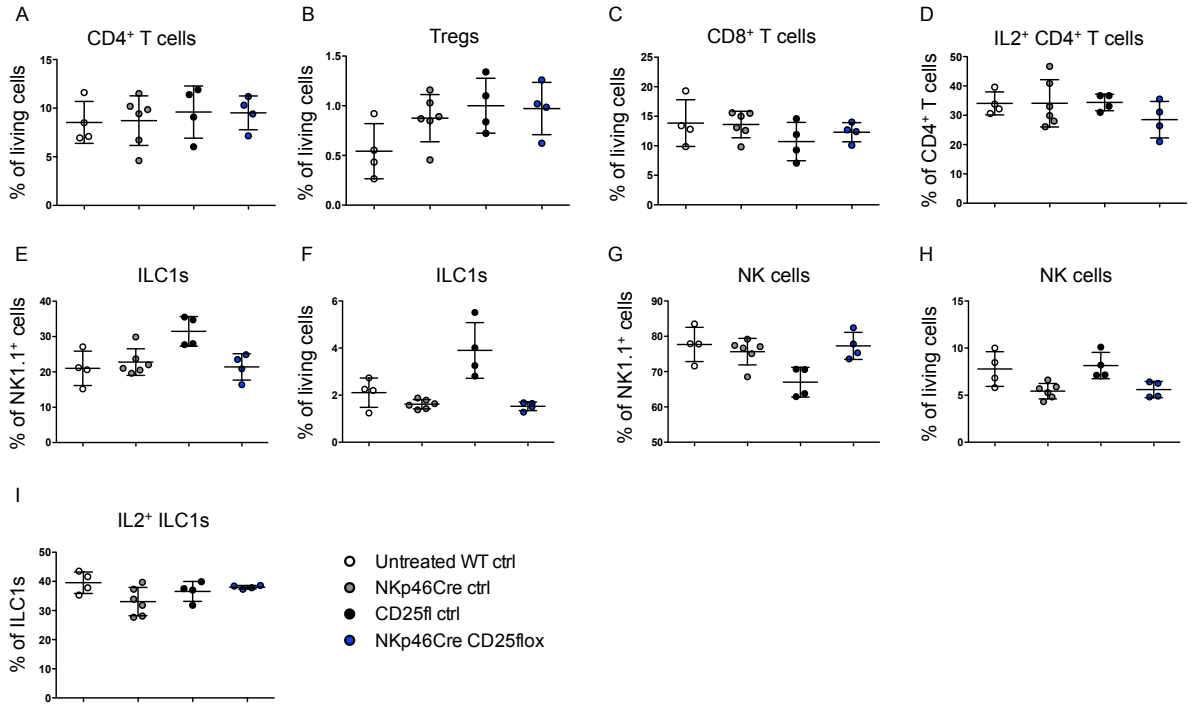

Figure 21: Lack of CD25 on ILC1s has moderate effects on IL2 production of CD4$^+$ T cells and ILC1s

Mice were treated with CCl_4 for 6 weeks and then left untreated for 3 weeks to analyze the reversal phase. Single cell suspensions from the liver were analyzed by flow cytometry. (A) Quantification of CD4 T cells, (B) Tregs, (C) CD8 T cells as percentage of living cells. (D) Percentage of IL2$^+$ cells within all CD4 T cells. (E-H) Frequency of ILC1s and NK cells within their compartment (E and G) or within all living cells (F and H). (I) Percentage of IL2$^+$ cells within all ILC1s. Cytokine production of CD4 T cells and ILC1s after 4h stimulation with Brefeldin A, PMA and Ionomycin at 37°C. Data is shown in mean ± SD from one experiment with n= 4-6 mice/group. No statistical differences were observed between relevant groups unless indicated as: *,P < 0,05; **,P < 0,005; ***,P < 0,0005.

6.8 Deletion of IL2 on NKp46$^+$ cells changes the innate and adaptive immune cell compartment during CCl_4-induced liver fibrosis

As the previous results showed a possible role for IL2 being produced by ILC1s, the next step was to perform the CCl_4-induced liver fibrosis in IL2fl x NKp46Cre mice after different time points. These mice lack IL2 specifically in NKp46$^+$ cells (Figure 22A). IL2 was efficiently depleted on ILC1s (Figure 22A and B). After 6 weeks of CCl_4-induced

liver fibrosis ILC1s of IL2fl x NKp46Cre mice show a decreased production of TNFα (Figure 22C). Other than that, the NK cell and ILC1 compartment is not changed (D-G). MPs and especially M2-like ($CD206^+$) MPs were increased in the IL2fl x NKp46Cre mice (Figure 22H and I). CD4 T cells, especially Tregs, are slightly reduced in these mice (Figure 22J-L) whereas NKT cells increase in percentage of living cells (Figure 22M). In addition to the shown data from flow cytometry, different inflammatory markers were analyzed by qPCR, serum parameter were analyzed to track liver damage and liver pathology was imaged by Picrosirius red and H&E stain but showed no major differences (data not shown).

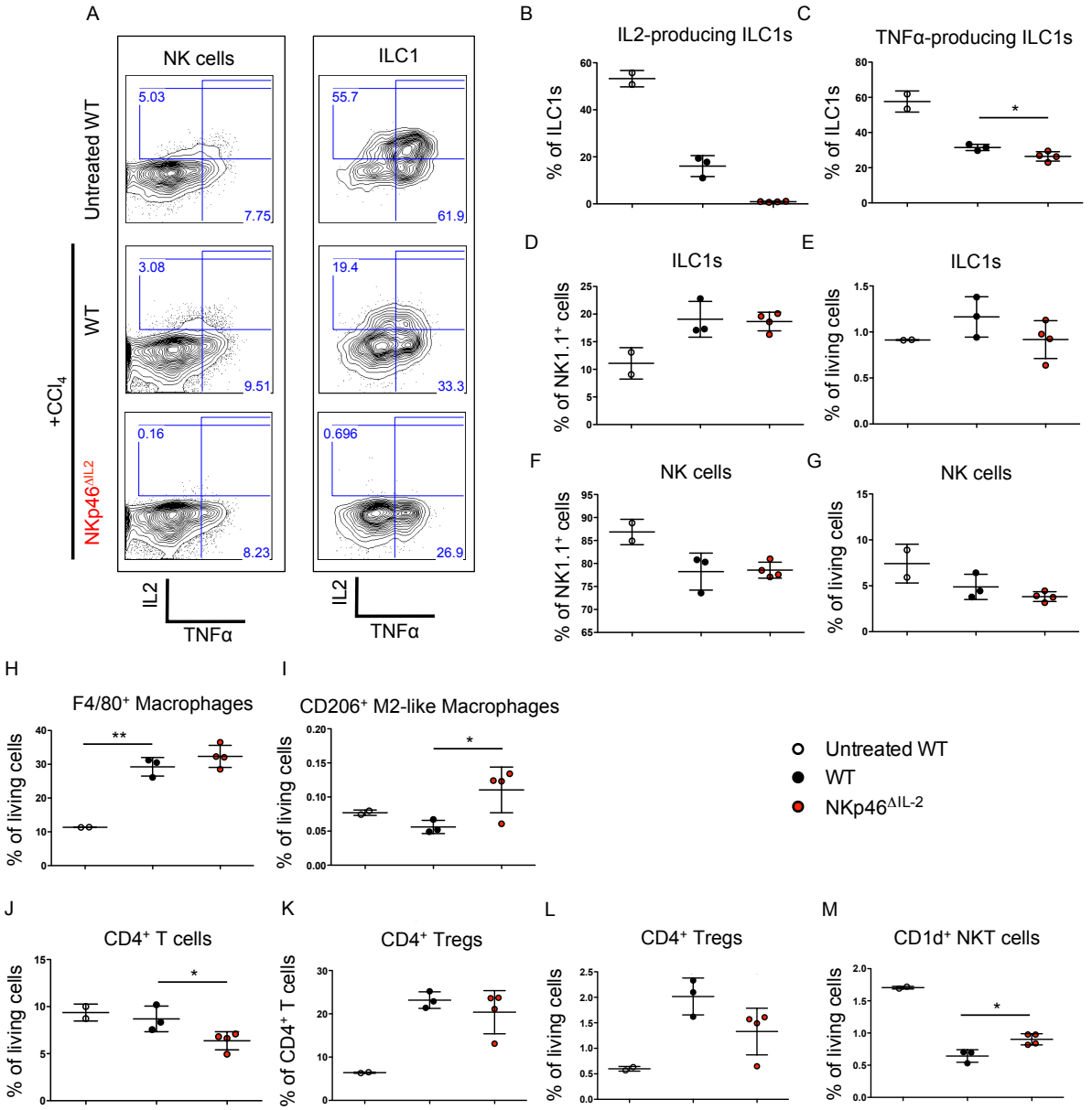

Figure 22: CCl_4-induced liver fibrosis leads to downregulation of ILC1-derived IL2

Mice were treated with CCl_4 for 6 weeks as described before. Single cell suspensions from the liver were analyzed by flow cytometry. (A) Representative FACS plots are shown to illustrate IL2 and TNFα expression on NK cells and ILC1s. (B and C) Quantification of IL2 (B) and TNFα (C) production by ILC1s shown in (A). (D-G) The ILC1 and NK cell compartment shown as percentage of $NK1.1^+$ cells (D and F) and as percentage of all living cells (E and G). (H and I) Frequency of all MPs (H) and M2-like MPs (I) within living cells. (J-M) Changes in the T cell compartment shown for CD4 T cells (J), Tregs (K and L) and NKT cells (M). Cytokine production of ILC1s was analyzed after 4h stimulation with Brefeldin A, PMA and Ionomycin at 37°C. Data is shown in mean ± SEM from one experiment with n= 2-3 mice/group. *,P < 0,05; **,P < 0,005; ***,P < 0,0005; ns, not significant

In the repetition of the experiment with younger (8 weeks old at start) female mice (preferably used in this model) changes in the cell compartments of T cells and ILCs of the liver were analyzed. The results from the first experiment could not be reproduced (data not shown). This might be due to the different age or sex of the mice. The experiments could be repeated using young female mice for optimal conditions, also including NKp46Cre x WT control mice.

To figure out a role in the reversal and by that tissue-healing phase of the disease, a 6 weeks induction plus 3 weeks reversal-experiment was performed. IL2 might be important during that phase to promote Treg proliferation and survival. The group 1 ILC compartment and the T cell compartment showed no significant differences (Figure 23A-F). The cytokine production of ILCs and T cells was not altered (data not shown). Nevertheless, there was a tendency that IL2fl x NKp46Cre mice have less $Gr1^+$ cells and more M1-like MPs (Figure 23G and H). As a summary, IL2 from $NKp46^+$ cells might have effects on myeloid cells, but not on T cells and their cytokine production during the reversal phase of fibrosis.

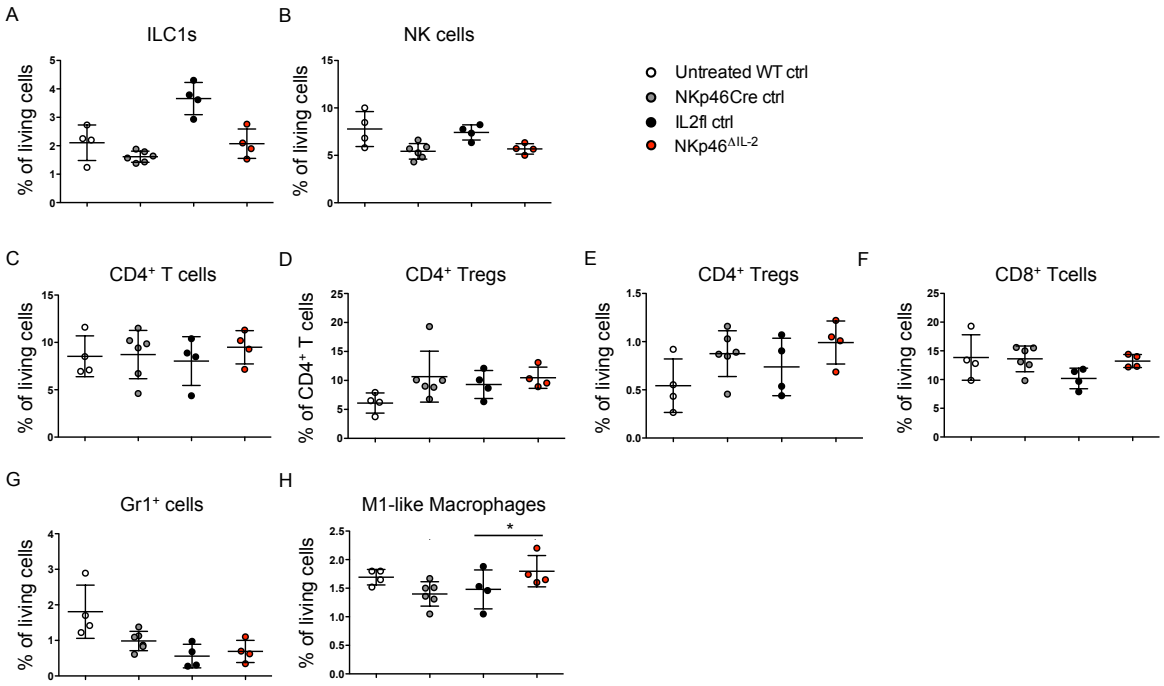

Figure 23: Lack of IL2 by ILC1s leads to a moderate change in the myeloid compartment during the reversal phase of CCl_4-induced liver fibrosis

Mice were treated with CCl_4 for 6 weeks and then left untreated for 3 weeks to analyze the reversal phase. Single cell suspensions from the liver were analyzed by flow cytometry. (A and B) Group 1 ILCs are quantified as percentage of living cells. (C-F) The T cell compartment shown as CD4 T cells in percentage of living cells (C), Tregs as percentage of all CD4 T cells (D) and of living cells (E) and CD8 T cells as percentage of living cells (F). (G and H) Analysis of the myeloid compartment, here $Gr1^+$ cells (G) and M1-like MPs (H). Data is shown in mean ± SD from one experiment with n= 4-6 mice/group. No statistical differences were observed between relevant groups unless indicated as: *,P < 0,05.

6.9 Lack of group 1 ILCs changes the innate immune cell compartment in the reversal phase of CCl_4-induced liver fibrosis

As the deletion of the cytokine IL2 or of the receptor subunit alpha in group 1 ILCs showed only subtle differences in the development and recovery of CCl_4-induced liver fibrosis, the next step was to investigate the overall role of group 1 ILCs in the tissue healing phase. After 6 weeks of treatment mice were left untreated for the reversal phase 3 weeks later. The analysis via flow cytometry shows that mice lacking $NKp46^+$ cells have slightly more $CD4^+IL17^+$ cells (Figure 24A). Furthermore, there were less $IL2^+$ and $IFN\gamma^+$ CD4 T cells in the NKp46Cre x iDTA group (Figure 24B and C). There were no differences detected in the T cell compartment (data not shown). Interestingly, $Gr1^+$ cells (Figure 24D), M2-like MPs (Figure 24E) and DCs (Figure 24F) were significantly increased in NKp46Cre x iDTA mice. According to these results, NK cells

and ILC1s might play an important role in regulating the myeloid compartment in the reversal process of CCl_4-induced liver fibrosis. As a next step, it would be interesting to investigate the role of these cells in the acute stage of disease.

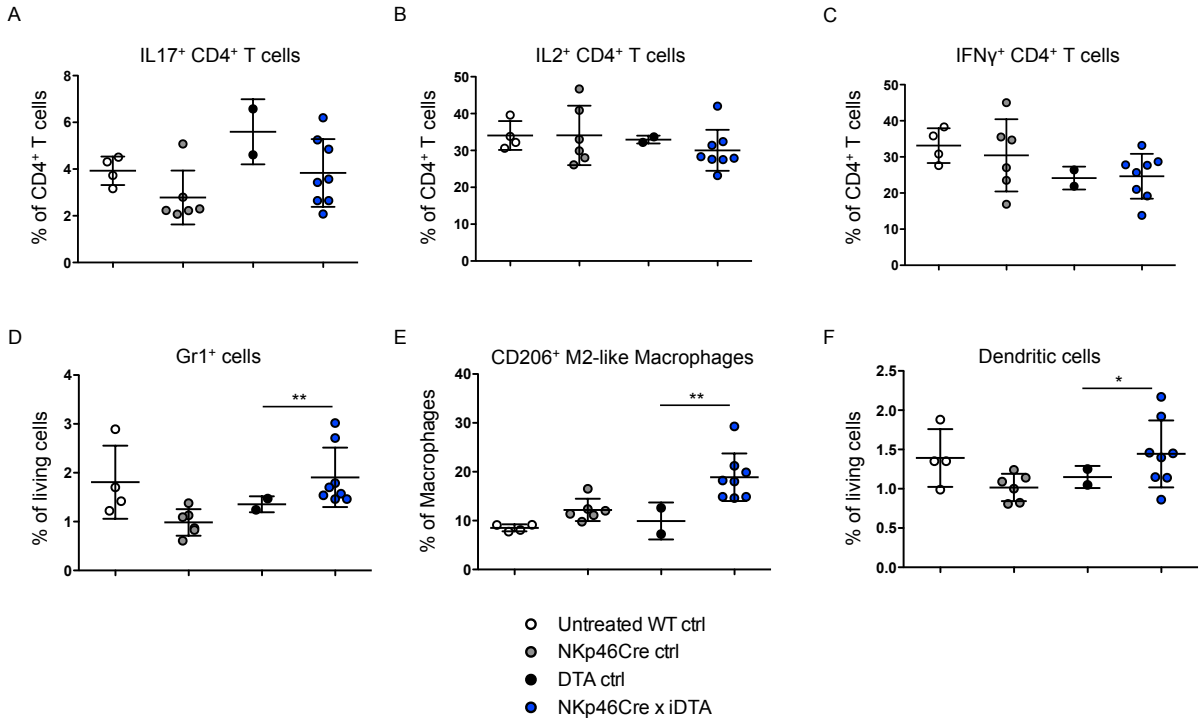

Figure 24: Lack of NK cells and ILC1s under CCl_4-induced liver fibrosis changes the myeloid compartment

Mice were treated with CCl_4 for 6 weeks and then left untreated for 3 weeks to analyze the reversal phase. Single cell suspensions from the liver were analyzed by flow cytometry. (A-C) Cytokine profile of CD4 T cells show the amount of $IL17A^+$ (A), $IL2^+$ (B) and $IFN\gamma^+$ (C) cells within all CD4 T cells. Cytokine production of CD4 T cells after 4h stimulation with Brefeldin A, PMA and Ionomycin at 37°C. (D-F) Quantification of the innate lymphocyte compartment showing changes in $Gr1^+$ cells (D), $CD206^+$ M2-like MPs (E) and DCs (F). Data is shown in mean ± SD from one experiment with n= 2-8 mice/group. ns, not significant or as indicated. *,P < 0,05; **,P < 0,005; ***,P < 0,0005; ns, not significant

7 Discussion

Studying liver diseases in humans remains a challenging field as many factors influence the health state of the liver. As previously described, human liver diseases are often diagnosed at a late stage and mainly by chance during a routine check-up. The initial cause of the disease is difficult to identify for most of the cases. Therefore, researcher established mouse models that closely resemble human diseases. By now, there are several widely accepted mouse models available to study for example liver fibrosis, NASH and HCC development. Those established models support the finding of new therapeutical targets that can ameliorate at least some of the diverse liver diseases (Farrell et al., 2019). A major step in understanding acute and chronic inflammation is to investigate how the immune compartments are regulated under inflammatory conditions. Cytokines are proteins that can regulate immune cells by signaling via the corresponding receptor. The cytokine receptor can exist of more than one subunit. This is an important mechanism to regulate the response of the immune cell as the different subunits can have different affinities towards the cytokine. One example for this is IL2. It was shown that its receptor IL2R consists of three subunits, CD25, CD122 and CD132. Only the combination of all three has the highest affinity towards IL2. One subunit of the IL2R, CD25, was shown to be expressed by different cell types like T cells, DCs and ILCs (Gasteiger, Hemmers, Bos, et al., 2013; Li et al., 2016). Understanding IL2 signaling in ILCs could help to understand their regulation. In this study, the major focus was on understanding the role of group 1 ILCs in the course of different liver diseases, mainly NASH and HCC development. Early studies reported on the role of NK cells and recent studies also involve first reports about the role of ILC1s, especially in adipose tissue (Michelet et al., 2018; O'Sullivan et al., 2016; Wensveen et al., 2015). The models of diet-induced NASH and HCC and toxin-induced fibrosis were the focus of this study. The first experiments were performed by using the model of long-term CD-HFD feeding and thereby inducing NASH and HCC. In general, both compartments of group 1 ILCs showed a higher proliferation whereas the absolute numbers were not altered. That might be due to a related higher apoptosis rate happening at the same time and thereby compensating the proliferation rate. It was shown before that human NK cells that target tumor cells *in vitro* undergo apoptosis which is facilitated via NCR activation and FasL release (Poggi et al., 2005).

Group 1 ILCs might also further contribute to the course of liver disease by a decrease of their original function, shown as an overall decreased cytokine production after CD-

HFD. This dysfunctional phenotype was previously described in NK cells from obese mice or patients (Michelet et al., 2018). They show that NK cells from obese mice take up lipids which limits their anti-tumor capacity. Based on these observations it could be tested in upcoming experiments if NK cells and ILC1s similarly take up lipids during CD-HFD.

Another mechanism to regulate and limit the response of NK cells and ILC1s is the restriction of access to IL2 by Tregs (Gasteiger, Hemmers, Bos, et al., 2013; Gasteiger, Hemmers, Firth, et al., 2013). Further experiments were done with a Cre-specific knock-out for the IL2 gene to study a possible role of IL2 being produced by group 1 ILCs that express NKp46. The first set of experiments revealed differences as the serum parameters and tumor incidence of the knock-out mice showed a slightly milder phenotype compared to WT control mice. A second run of this experiment was analyzed at an earlier time point with the idea that the initiation of tumor development can be captured. No changes and also no tumors could be observed at this earlier time point (6 months compared to 8 months in the first experiment). One possible explanation could be that the chosen time point of analysis was too early and the disease did not develop yet. Therefore, based on the preliminary data obtained here, potential repeat experiments should be analyzed exactly at the same time point like the first experiment. A major advantage of this model is that the status of fibrosis can be tracked with the help of the serum parameters by taking a small sample of blood from the mice. The exact time point of analysis can then be adapted to the first set of experiments.

Further experiments were performed at earlier time points and in the model of high-carb with or without high-fat diet to study the onset of NASH and the contribution of group 1 ILCs. ILC1s showed slightly elevated proliferation and upregulated CD25. CD25 is the IL2Rα domain and was shown before to be regulated during HCC (Cabrera et al., 2012). It is also widely used as a disease activity marker and an upregulated soluble factor in the sera of patients with autoimmune diseases like SLE (systemic lupus erythematosus), RA (rheumatoid arthritis) and SS (Sjogren´s syndrome) (Campen et al., 1988; Diamant et al., 1991).

Another widely accepted model for inducing liver fibrosis and NASH is the oral gavage of CCl_4 (Y. O. Kim et al., 2017). It was used in this study to investigate a possible role for group 1 ILCs in the onset and development of NASH with a less time-consuming

model that is very liver-specific and thereby excludes secondary effects. Furthermore, the quick onset of disease also allows to study the reversal phase of disease as the liver recovers once the treatment is stopped. ILC1s upregulate CD25 in the progression of disease and expand and downregulate KLRG1 in the reversal phase. It was described before that NKp46^{+} cells can get activated via NKp46 ligands and kill activated hepatic stellate cells (HSC) during fibrosis (Gur et al., 2012). To prevent tissue damage, group 1 ILCs may need a tight regulation. The regulation might be accomplished through differential expression of KLRG1 and CD25, which would explain the highly diverse expression pattern for activation markers (KLRG1) or cytokine receptors (CD25). It was just recently shown that liver ILC1s quickly upregulate CD25 after acute CCl_4 induction (Nabekura et al., 2019). Here, we found that CD25 is regulated during inflammation in the liver. Nevertheless, the functions of ILC1s in acute versus chronic tissue damage and inflammation can be different and still need to be investigated in further detail. The regulation of CD25 also hints towards the previously mentioned competition for IL2 between ILC1s and other cells in the acute and chronic phase of disease. A high expression of CD25, as it increases affinity of the trimeric receptor, does increase the chance to signal for IL2 compared to other cells expressing less CD25.

Toxin-induced liver fibrosis was performed in MMP3 KO mice to investigate the hepatic ILC compartment in additional experimental models that may more closely mimic the human disease. MMPs can contribute to the development of fibrosis by their potential to produce components of the ECM (Robert et al., 2016). MMP3 and other MMPs like MMP8 were shown to be associated with several liver diseases like HCC, fibrosis and hepatitis (Duarte et al., 2015).

FACS Analysis revealed a differential role of ILC1s, mainly expanding in the reversal phase whereas they generally upregulate CD25 during progression. This upregulation of CD25 in the progression of fibrosis was also observed in the CCl_4 model. MMP3 might have an effect on the proliferation and CD25 expression of ILC1s as the KO mice show less Ki67 and CD25 expression in the progression and more Ki67 and CD25 in the reversal phase. It was shown before that CD25 can be cleaved by another MMP, MMP9 in the cornea of mice (De Paiva et al., 2009). This shows that MMPs in general are able to regulate CD25 surface expression and hints towards a possible role for MMP3 in the regulation of CD25 expression in liver ILC1s during fibrosis.

To further identify the role of ILC1s during fibrosis and NASH, experiments were done with a knockout of CD25 in NKp46-expressing cells. The idea was to test the effect and function of CD25 expression by ILC1s during fibrosis. The only cell-intrinsic effect seen after 3 months of treatment with CCl_4 was the elevated production of IL2 in cells lacking the IL2Rα. This may suggest that CD25 has a regulatory function in ILC1s and suppresses their IL2 production. Cell extrinsic effects were observed in the downregulated IL17 production by CD4 T cells. This could be caused by the fact that ILC1s produce more IL2 and thereby support Treg proliferation and survival. IL2 could also directly inhibit Th17 differentiation, as previously suggested (Laurence et al., 2007; Liao et al., 2011). Further studies should investigate the regulatory mechanisms between CD4 T cells, Tregs and ILC1s. Another interesting question is the location of these cell types within the heterogeneous liver microenvironment to visualize potential direct cell-cell contact-dependent regulation. This could be tested with histological methods.

Additional fibrosis experiments with IL2fl x NKp46Cre mice were performed to investigate the effect of IL2 from ILC1s on a cell-intrinsic and –extrinsic basis. After analyzing these cells by flow cytometry only minor changes in the cell compartments were observed. This could be explained by the production of IL2 from ILC1s only being important locally to regulate neighboring cells. In that case, CD4 T cells might compensate the missing IL2 production by ILC1s by producing more IL2 only locally, which is difficult to distinguish by flow cytometry because it only allows the analysis of the whole liver. This observation shows again the importance of histology to figure out a local regulation between innate and adaptive lymphocytes.

To investigate the role of hepatic group ILC1s in the liver, additional experiments were done with mice that lack all NKp46-expressing cells. Some studies show a beneficial role for NK cells in the course of NASH (Tosello-Trampont et al., 2016), whereas others report a devastating role in adipose tissue (Wensveen et al., 2015). It is generally known that NK cells contribute to the inflammatory response by producing IFNγ but the precise effect is still largely unclear. So far, no experiments were done with the genetic model of group 1 ILC depletion via DTA but rather by using antibodies (Wensveen et al., 2015) or diphteria toxin (Tosello-Trampont et al., 2016). The results show a slightly altered cytokine expression pattern for CD4 T cells. The major difference was in the myeloid compartment. Granulocytes, M2-like MPs and DCs were significantly increased. This can be caused by interaction and regulation between different innate

cell compartments that compensate for the lack of group 1 ILCs. DCs can also produce IFNγ although to a much lower degree than NK cells (Vremec et al., 2007). This study also showed a slight effect of NK cells on IFNγ production by DCs. The increase in M2-like MPs might resemble a milder phenotype of the disease. M2-like MPs typically expand in the reversal phase as they are known to be responsible for tissue healing and being anti-inflammatory (Mills et al., 2000). Further studies should focus on the interaction of NK/ILC1 with the myeloid compartment to reveal whether these effects are a direct or indirect consequence of the lack of group 1 ILCs in this setting.

As shown in this work, studying the IL2 function and effects on innate and adaptive lymphocytes remains a challenging field with many open questions that need state-of-the-art techniques to be answered step-by-step. Depletion of CD25 or IL2 in group 1 ILCs can affect both innate and adaptive lymphocytes in the setting of HFD and liver fibrosis. Unravelling the regulatory mechanisms of IL2 signaling might then provide new therapeutic targets for the intervention of HFD and fibrosis.

8 References

Brunt, E. M. (2004). Nonalcoholic Steatohepatitis. *Seminars in Liver Disease*, *24*(1), 3–20. https://doi.org/10.1055/s-2004-823098

Cabrera, R., Fitian, A. I., Ararat, M., Xu, Y., Brusko, T., Wasserfall, C., Atkinson, M. A., Liu, C., & Nelson, D. R. (2012). Serum levels of soluble CD25 as a marker for hepatocellular carcinoma. *Oncology Letters*, *4*(4), 840–846. https://doi.org/10.3892/ol.2012.826

Campen, D. H., Horwitz, D. A., Quismorio, F. P., Ehresmann, G. R., & John Martin, W. (1988). Serum levels of interleukin-2 receptor and activity of rheumatic diseases characterized by immune system activation. *Arthritis & Rheumatism*, *31*(11), 1358–1364. https://doi.org/10.1002/art.1780311103

Castillo, E. F., Stonier, S. W., Frasca, L., & Schluns, K. S. (2009). Dendritic Cells Support the In Vivo Development and Maintenance of NK Cells via IL-15 Trans-Presentation. *The Journal of Immunology*, *183*(8), 4948–4956. https://doi.org/10.4049/jimmunol.0900719

Corbin, K. D., & Zeisel, S. H. (2012). Choline metabolism provides novel insights into nonalcoholic fatty liver disease and its progression. *Current Opinion in Gastroenterology*, *28*(2), 159–165. https://doi.org/10.1097/MOG.0b013e32834e7b4b

de Meijer, V. E., Sverdlov, D. Y., Popov, Y., Le, H. D., Meisel, J. A., Nosé, V., Schuppan, D., & Puder, M. (2010). Broad-Spectrum Matrix Metalloproteinase Inhibition Curbs Inflammation and Liver Injury but Aggravates Experimental Liver Fibrosis in Mice. *PLoS ONE*, *5*(6), e11256. https://doi.org/10.1371/journal.pone.0011256

De Paiva, C. S., Yoon, K.-C., Pangelinan, S. B., Pham, S., Puthenparambil, L. M., Chuang, E. Y., Farley, W. J., Stern, M. E., Li, D.-Q., & Pflugfelder, S. C. (2009). Cleavage of functional IL-2 receptor alpha chain (CD25) from murine corneal and conjunctival epithelia by MMP-9. *Journal of Inflammation (London, England)*, *6*, 31. https://doi.org/10.1186/1476-9255-6-31

Deng, T., Liu, J., Deng, Y., Minze, L., Xiao, X., Wright, V., Yu, R., Li, X. C., Blaszczak, A., Bergin, S., DiSilvestro, D., Judd, R., Bradley, D., Caligiuri, M., Lyon, C. J., & Hsueh, W. A. (2017). Adipocyte adaptive immunity mediates diet-induced adipose

inflammation and insulin resistance by decreasing adipose Treg cells. *Nature Communications*, *8*, 1–11. https://doi.org/10.1038/ncomms15725

Diamant, M., Tvede, N., Prause, J. U., Oxholm, P., Diamant', M., Tvede', N., Prause2, J. U., & Oxholm', P. (1991). Soluble Interleukin-2 Receptors in Serum from Patients with Primary Sjögren's Syndrome. *Scandinavian Journal of Rheumatology*, *20*(5), 370–372. https://doi.org/10.3109/03009749109096814

Duarte, S., Baber, J., Fujii, T., & Coito, A. J. (2015). Matrix metalloproteinases in liver injury, repair and fibrosis. *Matrix Biology : Journal of the International Society for Matrix Biology*, *44–46*, 147–156. https://doi.org/10.1016/j.matbio.2015.01.004

Farrell, G., Schattenberg, J. M., Leclercq, I., Yeh, M. M., Goldin, R., Teoh, N., & Schuppan, D. (2019). Mouse Models of Nonalcoholic Steatohepatitis: Toward Optimization of Their Relevance to Human Nonalcoholic Steatohepatitis. *Hepatology*, *69*(5), 2241–2257. https://doi.org/10.1002/hep.30333

Fasbender, F., Widera, A., Hengstler, J. G., & Watzl, C. (2016). Natural killer cells and liver fibrosis. *Frontiers in Immunology*, *7*(JAN), 1–7. https://doi.org/10.3389/fimmu.2016.00019

Gasteiger, G., Fan, X., Dikiy, S., Lee, S. Y., & Rudensky, A. Y. (2015). Tissue residency of innate lymphoid cells in lymphoid and nonlymphoid organs. *Science*, *350*(6263), 981–985. https://doi.org/10.1126/science.aac9593

Gasteiger, G., Hemmers, S., Bos, P. D., Sun, J. C., & Rudensky, A. Y. (2013). IL-2–dependent adaptive control of NK cell homeostasis. *The Journal of Experimental Medicine*, *210*(6), 1179–1187. https://doi.org/10.1084/jem.20122571

Gasteiger, G., Hemmers, S., Firth, M. A., Floc'h, A. Le, Huse, M., Sun, J. C., & Rudensky, A. Y. (2013). IL-2-dependent tuning of NK cell sensitivity for target cells is controlled by regulatory T cells. *Journal of Experimental Medicine*, *210*(6), 1065–1068. https://doi.org/10.1084/jem.20122462

Gasteiger, G., & Rudensky, A. Y. (2014). Interactions between innate and adaptive lymphocytes. *Nature Reviews Immunology*, *14*(9), 631–639. https://doi.org/10.1038/nri3726

Gordon, J., & Maclean, L. D. (1965). A Lymphocyte-stimulating Factor produced in vitro. *Nature*, *208*(5012), 795–796. https://doi.org/10.1038/208795a0

Granucci, F., Feau, S., Angeli, V., Trottein, F., & Ricciardi-Castagnoli, P. (2003). Early IL-2 Production by Mouse Dendritic Cells Is the Result of Microbial-Induced Priming. *The Journal of Immunology*, *170*(10), 5075–5081. https://doi.org/10.4049/jimmunol.170.10.5075

Gur, C., Doron, S., Kfir-Erenfeld, S., Horwitz, E., Abu-tair, L., Safadi, R., & Mandelboim, O. (2012). NKp46-mediated killing of human and mouse hepatic stellate cells attenuates liver fibrosis. *Gut*, *61*(6), 885–893. https://doi.org/10.1136/gutjnl-2011-301400

Han, J. M., Wu, D., Denroche, H. C., Yao, Y., Verchere, C. B., & Levings, M. K. (2015). IL-33 Reverses an Obesity-Induced Deficit in Visceral Adipose Tissue ST2 $^{+}$ T Regulatory Cells and Ameliorates Adipose Tissue Inflammation and Insulin Resistance. *The Journal of Immunology*, *194*(10), 4777–4783. https://doi.org/10.4049/jimmunol.1500020

Haybaeck, J., Zeller, N., Wolf, M. J., Weber, A., Wagner, U., Kurrer, M. O., Bremer, J., Iezzi, G., Graf, R., Clavien, P. A., Thimme, R., Blum, H., Nedospasov, S. A., Zatloukal, K., Ramzan, M., Ciesek, S., Pietschmann, T., Marche, P. N., Karin, M., … Heikenwalder, M. (2009). A Lymphotoxin-Driven Pathway to Hepatocellular Carcinoma. *Cancer Cell*, *16*(4), 295–308. https://doi.org/10.1016/j.ccr.2009.08.021

Heink, S., Yogev, N., Garbers, C., Herwerth, M., Aly, L., Gasperi, C., Husterer, V., Croxford, A. L., Möller-Hackbarth, K., Bartsch, H. S., Sotlar, K., Krebs, S., Regen, T., Blum, H., Hemmer, B., Misgeld, T., Wunderlich, T. F., Hidalgo, J., Oukka, M., … Korn, T. (2017). Trans-presentation of IL-6 by dendritic cells is required for the priming of pathogenic TH17 cells. *Nature Immunology*, *18*(1), 74–85. https://doi.org/10.1038/ni.3632

Kim, J. M., Rasmussen, J. P., & Rudensky, A. Y. (2007). Regulatory T cells prevent catastrophic autoimmunity throughout the lifespan of mice. *Nature Immunology*, *8*(2), 191–197. https://doi.org/10.1038/ni1428

Kim, Y. O., Popov, Y., & Schuppan, D. (2017). *Optimized Mouse Models for Liver Fibrosis* (pp. 279–296). Humana Press, New York, NY. https://doi.org/10.1007/978-1-4939-6786-5_19

Laurence, A., Tato, C. M., Davidson, T. S., Kanno, Y., Chen, Z., Yao, Z., Blank, R. B.

B., Meylan, F., Siegel, R., Hennighausen, L., Shevach, E. M., & O'Shea, J. J. J. (2007). Interleukin-2 Signaling via STAT5 Constrains T Helper 17 Cell Generation. *Immunity*, *26*(3), 371–381. https://doi.org/10.1016/j.immuni.2007.02.009

Lee, S.-H., Fragoso, M. F., & Biron, C. A. (2012). Cutting edge: a novel mechanism bridging innate and adaptive immunity: IL-12 induction of CD25 to form high-affinity IL-2 receptors on NK cells. *Journal of Immunology (Baltimore, Md. : 1950)*, *189*(6), 2712–2716. https://doi.org/10.4049/jimmunol.1201528

Li, J., Lu, E., Yi, T., & Cyster, J. G. (2016). EBI2 augments Tfh cell fate by promoting interaction with IL-2-quenching dendritic cells. *Nature*, *533*(7601), 110–114. https://doi.org/10.1038/nature17947

Liao, W., Lin, J. X., Wang, L., Li, P., & Leonard, W. J. (2011). Modulation of cytokine receptors by IL-2 broadly regulates differentiation into helper T cell lineages. *Nature Immunology*, *12*(6), 551–559. https://doi.org/10.1038/ni.2030

Michelet, X., Dyck, L., Hogan, A., Loftus, R. M., Duquette, D., Wei, K., Beyaz, S., Tavakkoli, A., Foley, C., Donnelly, R., O'Farrelly, C., Raverdeau, M., Vernon, A., Pettee, W., O'Shea, D., Nikolajczyk, B. S., Mills, K. H. G., Brenner, M. B., Finlay, D., & Lynch, L. (2018). Metabolic reprogramming of natural killer cells in obesity limits antitumor responses. *Nature Immunology*, *19*(12), 1330–1340. https://doi.org/10.1038/s41590-018-0251-7

Mills, C. D., Kincaid, K., Alt, J. M., Heilman, M. J., & Hill, A. M. (2000). M-1/M-2 macrophages and the Th1/Th2 paradigm. *Journal of Immunology (Baltimore, Md. : 1950)*, *164*(12), 6166–6173. https://doi.org/10.4049/jimmunol.164.12.6166

Murakami, S. (2004). Soluble interleukin-2 receptor in cancer. *Frontiers in Bioscience : A Journal and Virtual Library*, *9*, 3085–3090. http://www.ncbi.nlm.nih.gov/pubmed/15353339

Nabekura, T., Riggan, L., Hildreth, A. D., O'Sullivan, T. E., & Shibuya, A. (2019). Type 1 Innate Lymphoid Cells Protect Mice from Acute Liver Injury via Interferon-γ Secretion for Upregulating Bcl-xL Expression in Hepatocytes. *Immunity*. https://doi.org/10.1016/j.immuni.2019.11.004

Narni-Mancinelli, E., Chaix, J., Fenis, A., Kerdiles, Y. M., Yessaad, N., Reynders, A., Gregoire, C., Luche, H., Ugolini, S., Tomasello, E., Walzer, T., & Vivier, E. (2011). Fate mapping analysis of lymphoid cells expressing the NKp46 cell surface

receptor. *Proceedings of the National Academy of Sciences of the United States of America*, *108*(45), 18324–18329. https://doi.org/10.1073/pnas.1112064108

O'Sullivan, T. E., Rapp, M., Fan, X., Weizman, O. El, Bhardwaj, P., Adams, N. M., Walzer, T., Dannenberg, A. J., & Sun, J. C. (2016). Adipose-Resident Group 1 Innate Lymphoid Cells Promote Obesity-Associated Insulin Resistance. *Immunity*, *45*(2), 428–441. https://doi.org/10.1016/j.immuni.2016.06.016

Poggi, A., Massaro, A.-M., Negrini, S., Contini, P., Zocchi, M. R., Yonehara, S., & Nagai, K. (2005). Tumor-induced apoptosis of human IL-2-activated NK cells: role of natural cytotoxicity receptors. *Journal of Immunology (Baltimore, Md. : 1950)*, *174*(5), 2653–2660. https://doi.org/10.4049/jimmunol.174.5.2653

Popov, Y., Sverdlov, D. Y., Sharma, A. K., Bhaskar, K. R., Li, S., Freitag, T. L., Lee, J., Dieterich, W., Melino, G., & Schuppan, D. (2011). Tissue transglutaminase does not affect fibrotic matrix stability or regression of liver fibrosis in mice. *Gastroenterology*, *140*(5), 1642–1652. https://doi.org/10.1053/j.gastro.2011.01.040

Robert, S., Gicquel, T., Victoni, T., Valença, S., Barreto, E., Bailly-Maître, B., Boichot, E., & Lagente, V. (2016). Involvement of matrix metalloproteinases (MMPs) and inflammasome pathway in molecular mechanisms of fibrosis. *Bioscience Reports*, *36*(4), e00360. https://doi.org/10.1042/BSR20160107

Rubin, L. A., Jay, G., & Nelson, D. L. (1986). The released interleukin 2 receptor binds interleukin 2 efficiently. *Journal of Immunology (Baltimore, Md. : 1950)*, *137*(12), 3841–3844. http://www.ncbi.nlm.nih.gov/pubmed/3023487

Scholten, D., Trebicka, J., Liedtke, C., & Weiskirchen, R. (2015). The carbon tetrachloride model in mice. *Laboratory Animals*, *49*(1_suppl), 4–11. https://doi.org/10.1177/0023677215571192

Schuppan, D., Ruehl, M., Somasundaram, R., & Hahn, E. G. (2001). Matrix as a Modulator of Hepatic Fibrogenesis. *Seminars in Liver Disease*, *21*(03), 351–372. https://doi.org/10.1055/s-2001-17556

Shimizu, J., Yamazaki, S., & Sakaguchi, S. (1999). Autoimmunity Between Tumor Immunity and T Cells: A Common Basis + CD4 + CD25 Induction of Tumor Immunity by Removing. In *J Immunol References* (Vol. 5211). http://www.jimmunol.org/content/163/10/http://www.jimmunol.org/content/163/10/

5211.full#ref-list-1

Spits, H., Artis, D., Colonna, M., Diefenbach, A., Di Santo, J. P., Eberl, G., Koyasu, S., Locksley, R. M., McKenzie, A. N. J., Mebius, R. E., Powrie, F., & Vivier, E. (2013). Innate lymphoid cells — a proposal for uniform nomenclature. *Nature Reviews Immunology*, *13*(2), 145–149. https://doi.org/10.1038/nri3365

Tosello-Trampont, A. C., Krueger, P., Narayanan, S., Landes, S. G., Leitinger, N., & Hahn, Y. S. (2016). NKp46+natural killer cells attenuate metabolism-induced hepatic fibrosis by regulating macrophage activation in mice. *Hepatology*, *63*(3), 799–812. https://doi.org/10.1002/hep.28389

Vremec, D., O'keeffe, M., Hochrein, H., Fuchsberger, M., Caminschi, I., Lahoud, M., & Shortman, K. (2007). Production of interferons by dendritic cells, plasmacytoid cells, natural killer cells, and interferon-producing killer dendritic cells. *Blood*, *109*, 1165–1173. https://doi.org/10.1182/blood-2006-05

Wensveen, F. M., Jelenčić, V., Valentić, S., Šestan, M., Wensveen, T. T., Theurich, S., Glasner, A., Mendrila, D., Štimac, D., Wunderlich, F. T., Brüning, J. C., Mandelboim, O., & Polić, B. (2015). NK cells link obesity-induced adipose stress to inflammation and insulin resistance. *Nature Immunology*, *16*(4), 376–385. https://doi.org/10.1038/ni.3120

Williams, A. T., & Burk, R. F. (1990). Carbon Tetrachloride Hepatotoxicity: An Example of Free Radical-Mediated Injury. In *SEMINARS IN LIVER DISEASE* (Vol. 10, Issue 4). https://www.thieme-connect.com/products/ejournals/pdf/10.1055/s-2008-1040483.pdf

Wolf, M. J., Adili, A., Piotrowitz, K., Abdullah, Z., Boege, Y., Stemmer, K., Ringelhan, M., Simonavicius, N., Egger, M., Wohlleber, D., Lorentzen, A., Einer, C., Schulz, S., Clavel, T., Protzer, U., Thiele, C., Zischka, H., Moch, H., Tschöp, M., … Heikenwalder, M. (2014). Metabolic activation of intrahepatic CD8+T cells and NKT cells causes nonalcoholic steatohepatitis and liver cancer via cross-talk with hepatocytes. *Cancer Cell*, *26*(4), 549–564. https://doi.org/10.1016/j.ccell.2014.09.003

Wolf, R. E., & Brelsford, W. G. (1988). Soluble interleukin-2 receptors in systemic lupus erythematosus. *Arthritis & Rheumatism*, *31*(6), 729–735. https://doi.org/10.1002/art.1780310605

Wuest, S. C., Edwan, J. H., Martin, J. F., Han, S., Perry, J. S. A., Cartagena, C. M., Matsuura, E., Maric, D., Waldmann, T. A., & Bielekova, B. (2011). A role for interleukin-2 trans-presentation in dendritic cell-mediated T cell activation in humans, as revealed by daclizumab therapy. *Nature Medicine*, *17*(5), 604–609. https://doi.org/10.1038/nm.2365

Yuan, D., Huang, S., Berger, E., Liu, L., Gross, N., Heinzmann, F., Ringelhan, M., Connor, T. O., Stadler, M., Meister, M., Weber, J., Öllinger, R., Simonavicius, N., Reisinger, F., Hartmann, D., Meyer, R., Reich, M., Seehawer, M., Leone, V., … Heikenwalder, M. (2017). Kupffer Cell-Derived Tnf Triggers Cholangiocellular Tumorigenesis through JNK due to Chronic Mitochondrial Dysfunction and ROS. *Cancer Cell*, *31*(6), 771-789.e6. https://doi.org/10.1016/j.ccell.2017.05.006

Zhou, L., Chu, C., Teng, F., Bessman, N. J., Goc, J., Santosa, E. K., Putzel, G. G., Kabata, H., Kelsen, J. R., Baldassano, R. N., Shah, M. A., Sockolow, R. E., Vivier, E., Eberl, G., Smith, K. A., & Sonnenberg, G. F. (2019). Innate lymphoid cells support regulatory T cells in the intestine through interleukin-2. *Nature*, *568*(7752), 405–409. https://doi.org/10.1038/s41586-019-1082-x

9 Appendix

Acknowledgments

[redacted]

Curriculum Vitae Christian Hessel

Address [redacted]

[redacted]

E-Mail: [redacted]

Place and date of birth: [redacted]

PhD thesis

since 05/2015 Johannes Gutenberg-University Mainz, performed at the Julius-Maximilians-University, Würzburg

Institute of Systems Immunology [redacted]

Subject: **Role of the Interleukin-2 pathways in hepatic innate lymphoid cells during steady state, fibrosis and hepatocellular carcinoma**

Publication [redacted]

Conferences Natural killer cell Symposium, Göttingen, 7th to 9th of October, 2015

T cell meeting, Marburg, 27th to 28th of June 2016

Spring school on Immunology, Ettal, 5th to 10th of March 2017

Undergraduate studies

10/2012-04/2015 Johannes Gutenberg-University, Mainz

Degree: Master of Science, Biology

Major subjects: Human and developmental genetics

Immunological master thesis at the Institute of Molecular Medicine, University medical center, Mainz in the group of [redacted]

04/2009-05/2012 Johannes Gutenberg-University, Mainz

Degree: Bachelor of Science, Biology

Eidesstattliche Erklärung

Hiermit versichere ich, dass ich die vorliegende Doktorarbeit selbstständig angefertigt und keine anderen als die angegebenen Hilfsmittel und Quellen in der Arbeit verwendet habe. Weiterhin bestätige ich, dass ich die vorliegende Arbeit, oder Teile davon, nicht als Arbeit in einer anderen Fakultät oder für eine andere Prüfung benutzt habe.

Mainz, 07.02.2021 _____

Christian Hessel